

QUANTUM CHROMODYNAMICS AND THE PRODUCTION
OF HADRONS AT LARGE TRANSVERSE MOMENTUM

by



Stavros Papadopoulos

A thesis submitted to the Faculty of Graduate Studies and Research
in partial fulfilment of the requirements
for the degree of Master of Science

Department of Physics
McGill University
Montreal, Quebec, Canada

May, 1979

LARGE TRANSVERSE MOMENTUM PRODUCTION OF HADRONS IN QCD

ABSTRACT

Inclusive meson production at large transverse momentum (p_T) in hadronic collisions is studied in the framework of Quantum Chromodynamics (improved parton model). Scale violations are included in the parton distribution and fragmentation functions; and the contributions from quark-quark, quark-gluon and gluon-gluon scattering to lowest order in the (running) coupling constant are added. The intrinsic transverse momentum of the partons relative to their parent hadrons is also taken into account. The general formalism is applied to pion production at large p_T in proton-proton collisions. CERN-ISR data are fairly well accounted for, but Fermilab data somewhat exceed the predictions. Possible subasymptotic effects contributing at relatively low p_T and energy are also discussed.

RESUME

On étudie la production inclusive des mésons à grande impulsion transverse (p_T) par les collisions hadroniques, dans le cadre de Chromodynamique Quantique (modèle de partons amélioré). Les violations de scaling sont incluses dans les fonctions de distribution et de fragmentation des partons; les contributions du plus bas ordre dans la constante (courante) de couplage dues aux collisions quark-quark, quark-gluon et gluon-gluon sont ajoutées. On tient compte de l'impulsion transverse intrinsèque des partons, relativement aux parents hadroniques. On applique ce formalism général à la production des pions à grands p_T dans les collisions proton-proton. Les données de CERN-ISR sont assez bien décrites mais celles de Fermilab excèdent quelque peu les prédictions. On discute aussi d'effets possibles sous-asymptotiques contribuant à des p_T et des énergies relativement basses.

ACKNOWLEDGEMENTS

This thesis is based on research work I did at McGill University during the Fall of 1977. The work could not be done without the knowledge I gained at this University and without the constant encouragement, collaboration and help of my supervisor, Professor A.P. Contogouris, whom I especially thank. I wish also to thank Dr. R. Gaskell for his collaboration during the course of the research.

The treatment of certain topics in this thesis has been influenced from helpful discussions with Mr. B. Campbell and Dr. J. Kripfganz at McGill University and with Professor S. Brodsky and Drs. R. Field and J. Owens at the 1978 Summer Workshop of the University of California, San Diego; it is my pleasure to thank them all.

TABLE OF CONTENTS

	Page
ABSTRACT	i
ACKNOWLEDGMENTS	iii
TABLE OF CONTENTS	iv
CHAPTER	
I Introduction	1
1.1 Large- p_T Physics	1
1.2 The Parton Model and e-h Inelastic Scattering	2
1.3 The BBK Model	6
1.4 The CIM Model	7
1.5 The Black-Box Model	8
1.6 Asymptotic Freedom. BBK Model with Scale Breaking	9
1.7 Parton Transverse Momenta	12
1.8 QCD as the Underlying QFT of Partons	13
II Large P_T Single Hadron Inclusive Production: General Formulation	16
2.1 The Inclusive Cross-Section with QCD and k_T Effects	16
2.2 Distribution and Fragmentation Functions from QCD	23
III Calculations and Comparison with Experiment	27
3.1 Calculations and Conclusions on k_T Effects	27
3.2 Comparison with experiment	30
IV Summary and Conclusions	32
4.1 Summary of our Work	32
4.2 Main Results from Large Transverse Momentum Correlations	33
4.3 Possible Corrections	34
4.4 Overall Conclusions	37
APPENDIX A: Details on Distribution and Fragmentation Functions	39
APPENDIX B: Sensitivity in Assumed Inputs	43
FOOTNOTES	46
TABLE	47
REFERENCES	48
FIGURE CAPTIONS	55

CHAPTER I

INTRODUCTION

1.1 Large- p_T Physics

The field of large transverse momentum (p_T) physics was born at ~ 1972. At that time early CERN-ISR experiments⁽¹⁾ indicated that the differential cross-section for single particle production with large p_T ($p_T \gtrsim 1$ GeV) in hadronic collisions is some orders of magnitude higher than what was expected from extrapolations of small p_T data. Those data ($p_T < 1$ GeV) are described by an inclusive cross-section of the form:

$$E \frac{d\sigma}{d^3p} \sim e^{-6p_T} \quad (1.1)$$

The CERN-ISR experimental data, suggested that a different production mechanism may be responsible for the large p_T yields. Actually the data could be explained in a hard scattering model, where the hadrons' constituents undergo an incoherent point-like scattering; this was in contrast to the coherent scattering picture of small p_T inclusive production, in which the initial hadrons participate as a whole.

This point of view was reinforced from the fact that the study of deep inelastic lepton (l) - hadron (h) scattering demonstrated that hadrons have an effective point-like constituent structure. The experimental data were well-explained in terms of the quark-parton model^{(2),(3)}, which could also be used to describe large p_T processes involving only hadrons. In this way large p_T hadron production and deep inelastic lepton production

were intimately related.

We shall briefly describe the quark-parton model below.

1.2 The Parton Model and e-h Inelastic Scattering

In the one photon exchange approximation (see Fig. 1) the inclusive electron scattering cross section from an unpolarized hadronic target is given by⁽⁴⁾

$$\frac{d\sigma}{d\Omega dE'} = \left(\frac{d\sigma}{d\Omega}\right)_{\text{Mott}} \left[W_2(\nu, Q^2) + 2W_1(\nu, Q^2) \tan^2 \frac{\theta}{2} \right] \quad (1.2)$$

where

$$\left(\frac{d\sigma}{d\Omega}\right)_{\text{Mott}} = \frac{4\alpha^2 E'^2}{Q^4} \cos^2 \frac{\theta}{2} \quad (1.3a)$$

and

$$Q^2 = -q^2 = -(k-k')^2 = 4EE' \sin^2 \frac{\theta}{2} \quad (1.3b)$$

$$\nu = \frac{q \cdot P}{M} = E - E' \quad ; \quad (1.3c)$$

$E(E')$ and θ are the initial (final) energy and the scattering angle of the electron in the lab frame; $k(k')$, q and P are the 4-momenta of the initial (final) electron, virtual photon and the target; M is the target mass and the electron mass is neglected.

W_1 and W_2 in (1.2) are in general functions of the two invariants ν and Q^2 of the process. They are called structure functions of the

target and represent a generalization of the form factors describing e-h elastic scattering.

Bjorken⁽⁵⁾ using the Adler sum rule⁽⁶⁾ obtained the following inequality for inelastic electron-nucleon scattering:

$$\int_0^{\infty} d\nu \left[W_2^{ep}(\nu, Q^2) + W_2^{en}(\nu, Q^2) \right] \geq \frac{1}{2} \quad (1.4)$$

The absence of Q^2 dependence on the R.H.S suggests that the total electron-nucleon scattering cross section corresponds to scattering of point-like objects.

Define

$$x = \frac{Q^2}{2M\nu} \quad (1.5)$$

and consider the limit $Q^2 \rightarrow \infty$, $\nu \rightarrow \infty$, $x = \text{fixed}$ (called Bjorken limit). Bjorken suggested⁽⁷⁾ that (1.4) can be understood if the structure functions in the integrand have the behaviour (called scaling):

$$W_2(\nu, Q^2) \xrightarrow{\text{Bj. Lim}} F_2(x); \quad (1.6)$$

then as $Q^2 \rightarrow \infty$

$$\int d\nu W_2(\nu, Q^2) = \int \frac{dx}{x} F_2(x) = Q^2 - \text{independent} \quad (1.7)$$

The scaling behaviour (1.6) and a similar behaviour for W_1

$$W_1(\nu, Q^2) \xrightarrow{\text{Bj. Lim}} F_1(x) \quad (1.8)$$

were consistent with subsequent experiments even at moderate values of Q^2 ($Q^2 > 1 \text{ GeV}^2$).

The scaling behaviour naturally arises in a simple constituent picture of the hadrons formulated by Feynman^{(2),(3)}, the parton model. According to this model the hadron consists of point-like (structureless) constituents, the partons. These are almost free, and carry a finite fraction of hadron's momentum. The electrons are scattered incoherently from the partons.

For the validity of this picture it is assumed that:

- (a) The impulse approximation can be applied: the constituents can be treated as free on a time scale (τ_{inter}) much shorter than the scale of their mutual strong couplings (τ_L):

$$\tau_{\text{inter}} \ll \tau_L \quad (1.8)$$

This condition is satisfied in a frame in which the hadron's momentum is very large.

- (b) The distribution of parton's momentum k_T transverse to the hadron's momentum has a sharp cutoff. In this case it can be shown that processes in which the virtual photon is absorbed by different partons cannot interfere; this leads to incoherent scattering. The sharp cutoff in the k_T -distribution is an assumption characteristic of the parton model.

Denote by $f_{i/H}(\xi)$ the probability density to find within a hadron H a parton of type i , with a fraction ξ of hadron's momentum. Then the above two conditions can be shown to imply^{(3),(8)}:

$$W_2^H(\nu, Q^2) = \sum_i \int_0^1 e_i^2 f_{i/H}(\xi) W_2^i d\xi = \sum_i \int_0^1 e_i^2 f_{i/H}(\xi) \delta(\nu - \frac{Q^2}{2M\xi}) d\xi$$

where e_i is the electric charge of the parton in units of the electron charge. Then,

$$vW_2^H(\nu, Q^2) \equiv F_2^H(x) = \sum_i e_i^2 x f_{i/H}(x) \Big|_{x = \frac{Q^2}{2M\nu}} \quad (1.9)$$

In this way the parton model easily leads to scaling behaviour.

Analysis of the experimental data indicated that the different types of partons can be identified with the (spin $\frac{1}{2}$) quark flavors encountered in hadronic spectroscopy. On the other hand it was found that about half of the momentum of the proton is carried by neutral partons (called gluons).

The parton model could be applied to other processes involving coupling of quarks with photons; e.g. electron - positron annihilation into hadrons ($e^+e^- \rightarrow X$) or lepton pair production ($h_1 + h_2 \rightarrow l^+l^- + X$). In general in these processes the differential cross-section can be factorized in three parts:

- i) the probability density $f_{i/h_1}(x)$ of finding inside an incoming hadron h_1 a quark of flavor i with fraction x of hadron's momentum (parton distribution function)
- ii) the point-like interaction of the quark i with the virtual photon
- iii) the probability density $G_{h_2/i}(z)$, for the scattered quark i to fragment into a hadron h_2 carrying a fraction z of quark's momentum (parton fragmentation function)^f1.

It is important to notice that measurement of the structure functions provides (through Eq. (1.9)) information about the quark distributions inside the hadron.

1.3 The BBK Model

The parton model was applied by Berman, Bjorken and Kogut (BBK) to purely hadronic reactions with large p_T yields⁽⁹⁾. Assuming that the large p_T hadron is produced in a single interaction between two incoming quarks they were led to the following form for the cross-section of the inclusive hadron reaction $A + B \rightarrow C + X$ (Fig. 2)^{(9),(10)}

$$E_C \frac{d\sigma}{d^3 p_C} (s, p_T, \theta_{cm}) = \frac{1}{\pi} \sum_{a,b,c} \int \int dx_a dx_b f_{a/A}(x_a) f_{b/B}(x_b) \frac{d\hat{\sigma}}{dt} \frac{G_{C/c}(z)}{z^2} \quad (1.10)$$

where θ_{cm} is the CM angle of the produced hadron C with large p_T , relative to the beam axis, and s the CM energy squared of the colliding hadrons.

For pp collisions the distribution functions $f_{a/A}(x_a)$ and $f_{b/B}(x_b)$ can be extracted from ep and vp deep inelastic scattering data, and the fragmentation functions $G_{C/c}(z)$ from ep and vp hadron production or from $e^+e^- \rightarrow \text{hadron} + X$.

In (1.10) $\frac{d\hat{\sigma}}{dt}$ represents the large angle scattering cross-section of the constituent subprocess $a + b \rightarrow c + d$. This cross-section carries information about the strong interactions.

The subprocess $a + b \rightarrow c + d$ was assumed to take place via single massless vector meson exchange and, as in a single photon exchange:

$$\frac{d\hat{\sigma}}{dt} \sim \hat{s}^{-2} \sim p_T^{-4} \quad (1.11)$$

Then if $f_{a/A}$, $f_{b/B}$ and $G_{C/c}$ satisfy exact scaling:

$$E_C \frac{d\sigma}{d^3 p_C} \sim \frac{1}{p_T^4} f(x_T, \theta_{cm}^*), \quad x_T = \frac{2p_T}{\sqrt{s}} \quad (1.12)$$

For fixed x_T and θ_{cm} , the above p_T^{-4} decrease of $E_C \frac{d\sigma}{d^3p_C}$ is much slower than that of the small p_T form (1.1), and it was in accord with the very early experiments⁽¹¹⁾. Later ISR data⁽¹¹⁾, however, on $pp \rightarrow \pi + X$ indicated a cross-section of the form (1.12), but with p_T^{-8} replacing p_T^{-4} . These data ruled out the naive (but attractive) scale invariant quark-quark (qq) scattering model and suggested various other models⁽¹²⁾. The most important of them were the constituent interchange model (CIM) and the black-box model.

1.4 The CIM Model

The constituent interchange model (CIM)^{(12),(13)} and a related model due to the Cambridge group⁽¹⁴⁾ explained the data by more complex scattering subprocesses as e.g.

$$qM \rightarrow qM', \quad qB \rightarrow qB', \quad q\bar{q} \rightarrow M\bar{M}, \quad (1.13)$$

where M (Meson), B (Baryon) indicate $q\bar{q}$ and qqq clusters. These subprocesses assumed scale invariant still lead to simple power-law behaviour:

$$E \frac{d\sigma}{d^3p} \sim \frac{1}{(p_T^2)^{n-2}} f(x_T, \theta_{cm}) \quad (1.14)$$

The p_T dependence is summarized by the following rule (called dimensional counting)⁽¹⁵⁾: n is the total number of elementary fields (quarks, electrons, photons etc) participating in the subprocess.

Since q, M, B have 1,2,3 constituents (elementary fields) respectively this rule leads to:

Subprocess	n	$E \frac{d\sigma}{d^3p} \sim$	
$qM \rightarrow qM'$	6	p_T^{-8}	(1.15a)
$q\bar{q} \rightarrow M\bar{M}$	6	p_T^{-8}	(1.15b)
$qB \rightarrow qB'$	8	p_T^{-12}	(1.15c)

Within this model the $pp \rightarrow \pi + X$ data could be interpreted using (1.15). It should be noted that the authors of Ref. 13 were advocating p_T^{-8} behaviour prior to its confirmation at ISR.

In the original version of the model problems of the normalization of each subprocess, the structure of the 'M' jets which are not necessarily the same as in lepton induced reactions and insufficient explanation for the absence of the qq subprocess, restricted the predictive power⁽¹⁶⁾. One could argue that this model did not provide the basic mechanism in large p_T physics. In its present form the model deserves special attention, as we shall discuss in Chapter IV.

1.5 The Black-Box Model

This model was introduced by Feynman, Field and Fox^{(17),(18)} and it is based on quark-quark scattering. The subprocess cross-section $\frac{d\hat{\sigma}}{d\hat{t}}$ in (1.10) was adjusted (black-box) so that the resulting inclusive cross-section fit the large p_T meson data. Assuming that the fundamental $qq \rightarrow qq$ subprocess contains a scale and behaves as

$$\frac{d\hat{\sigma}}{d\hat{t}} = h(\hat{t}/\hat{s}) \hat{s}^{-n} \quad (1.16)$$

(1.16) leads to

$$E \frac{d\sigma}{dp} \sim \frac{1}{(p_T^2)^n} f(x_T, \theta_{cm}) \quad (1.17)$$

clearly the choice $n = 4$ accounts for the data (p_T^{-8}) . One must also specify the absolute magnitude of $\frac{d\sigma}{dt}$, and an overall best fit was found with the expression:

$$\frac{d\sigma}{dt} = \frac{2.3 \times 10^3}{(-s \hat{t}^3)} \text{ mb GeV}^6 \quad (1.18)$$

The model was successful in accounting for ratios of single particle (meson) inclusive cross-sections as well as for jet cross-sections. It was in difficulty, however, to account for other data, particularly in relation with correlations for two large $-p_T$ hadrons in opposite directions.

The model has been considered as a "useful tool" in extracting information from the data, but not as a basic mechanism because of the lack of theoretical understanding of the form (1.18).

1.6 Asymptotic Freedom. BBK Model with Scale Breaking

Together with the development of several models⁽¹⁹⁾ various attempts were made to remove the difficulty of the BBK model to reproduce the experimental data.

These attempts stemmed from the understanding that if the interactions of partons are described by a renormalizable field theory (RFT) (i.e., with a dimensionless coupling constant) then the partons cannot

be treated as completely free; this because there is no time (and length) scale beyond which interactions can be ignored. In such a theory the partons will never be precisely structureless and point-like. A parton seen by a probe with a certain value of 4-momentum squared Q^2 , will reveal further substructure for a probe with higher Q^2 ⁽²⁰⁾⁻⁽²²⁾.

RFTs have been analyzed using renormalization group (RG) methods. The result of the analysis is that in such theories one expects violations of scaling. These violations are expressible more precisely in terms of the Q^2 -dependence of the moments.

$$M_n(Q^2) = \int_0^1 dx x^{n-2} F_2(x, Q^2) \quad (1.19)$$

of the structure function $F_2(x, Q^2)$. The predicted Q^2 -dependence of (1.19) for large values of Q^2 can be classified in two categories:

- (a) of inverse powers of Q^2 ; this occurs in conventional field theories (CFT), in which the renormalized coupling constant increases with Q^2 , as in QED or ϕ^4 -interaction.
- (b) of inverse powers of $\log Q^2$; this occurs in asymptotically free field theories (AFFT), in which the renormalized coupling constant decreases (logarithmically) with Q^2 (asymptotic freedom ⁽²³⁾), as in Yang-Mills gauge theories ⁽²⁴⁾.

AFFT are leading candidates for a theory of strong interactions; this because their property of asymptotic freedom gives credibility to the parton model and incorporates Bjorken scaling as an asymptotic phenomenon. It has been demonstrated ⁽²⁵⁾ that essentially the only asymptotically free theories are the non-abelian gauge theories of colored

quarks and gluons, Quantum Chromodynamics (QCD) ⁽²⁶⁾.

Scaling violations have now been observed in accurate deep inelastic scattering data ⁽²⁷⁾⁻⁽²⁹⁾.

Because of the definite QCD predictions and the experimental evidence it was of much interest to examine if the naive BBK model, reformulated to take into account scaling violations, could explain the features of the large p_T data.

The first study of this problem was made by Cahalan, Geer, Kogut and Susskind ⁽³⁰⁾. They used the scale-invariant parton model of Kogut and Susskind ^{(21),(22)} (intuitive but powerful extension of the naive parton model, incorporating the effects of scale invariant interactions) with logarithmic scale breaking in the distribution and fragmentation functions. They found, however, that their predictions were well below the data and that only at superhigh energies ($s = 6 \times 10^3 \text{ GeV}^2$) the model could agree with FNAL extrapolations. On the other hand, their form of scale breaking was a reasonable solution of QCD equations only for $x \sim 1$.

Another attempt was made by Hwa, Spiessback and Teper ⁽³¹⁾ who fit the data on deep inelastic eN scattering with a parametrization for the structure functions; this parametrization, extrapolated to high Q^2 within the BBK model, provided a fair account for the large p_T $pp \rightarrow \pi^0 + X$ data. Their parametrization, however, led to moments $M_n(Q^2)$ (Eq. (1.19)) decreasing like inverse powers of Q^2 , in disagreement with the QCD predictions.

In a further development, a model by Contogouris, Gaskell and Nicolaidis ⁽³²⁾, accounted for a number of QCD requirements and led to moments $M_n(Q^2)$ asymptotically behaving as inverse powers of $\log Q^2$.

This model provided a good understanding of the experimental data on single particle (meson) inclusive cross-sections and two particle correlations⁽³³⁾.

However, among the basic difficulties of, and objections to, the approach of Refs. 31, 32 and related work^{(33),(34)} are the following:

- i) The value of the strong coupling constant required to fit the data is higher by a factor of ~ 3 than the now accepted value of the running coupling constant of QCD.
- ii) The scale violation is stronger than that predicted by QCD, and, in general, the quark distributions are not deduced as solutions of QCD conditions.

1.7 Parton Transverse Momenta

In most of the early applications of the parton model the transverse momenta of partons (k_T) were assumed to be negligible.

Experimental results, however, like the wide transverse momentum distribution of massive lepton pairs⁽³⁵⁾⁻⁽³⁷⁾ and the lack of coplanarity of the away particles with respect to the beam-trigger plane⁽³⁸⁾⁻⁽⁴⁰⁾ (p_{out} distributions) indicated that the partons' transverse momenta have important effects and should not be neglected. These k_T effects have been the subject of many investigations⁽⁴¹⁾⁻⁽⁴⁵⁾.

As first pointed out by Combridge⁽⁴⁴⁾, the transverse momentum of the parton is biased in the direction of the detector. The reason is that because the cross-section falls off so rapidly with increasing trigger's p_T , configurations in which part of the p_T is supplied by the partons are favored. Roughly speaking the net effect corresponds to a translation (of order $\langle k_T \rangle$) of the inclusive cross-section curve, towards

the positive p_T axis; this affects both the magnitude and the shape of the cross-section, especially in the small p_T region (2-4 GeV).

Thus if k_T effects are introduced in the single particle cross-section the agreement with the data is expected to improve.

1.8 QCD as the Underlying QFT of Partons

In all the applications of the parton model discussed so far the effect of gluons was also neglected.

Another difficulty of all the models based only on qq scattering, is that they predict considerably more positive than negative hadrons on the away side. In p-p collisions at $\sqrt{s} = 53$ GeV and a trigger π^0 at $\theta_{cm} = 90^\circ$ and $p_T = 3$ GeV, the Black-Box model, for example, predicts 50% more positive than negative hadrons on the away side with $p_T > 1.5$ GeV⁽⁴⁶⁾; data from ISR show about equal numbers. This is one of the experimental indications that the recoiling away-side parton is not always a quark, but sometimes a neutral constituent (a gluon).

On the other hand, in QCD determinations of the scale breaking of quark distributions, gluon effects are inseparable and cannot be neglected. Therefore, a consistent QCD treatment of large p_T phenomena requires also quark-gluon (qg) and gluon-gluon (gg) scattering subprocesses. These subprocesses have been investigated and an important conclusion⁽⁴⁷⁾⁻⁽⁴⁹⁾ is that at $p_T \approx 2-5$ GeV production of hadrons via qg and gg scattering is very significant.

These considerations suggest that an approach based on QCD and taking into account the effects of partons' transverse momenta (k_T) may explain the main features of large p_T meson production.

The purpose of our work is to study the basic hadronic process $p + p \rightarrow \pi^0 + X$ (and $p + p \rightarrow \frac{1}{2} (\pi^+ + \pi^-) + X$) in the framework of parton-parton scattering using the following ingredients:

- i) The QCD running coupling constant $\alpha_s(Q^2)$.
- ii) Quark and gluon distribution functions satisfying, to a good approximation, all the QCD requirements and fitting the electroproduction and neutrino production data.^{(50), (51)}
- iii) All the hard scattering QCD subprocesses qq , qg and gg .
- iv) Intrinsic k_T distributions of partons inside a hadron (and of hadrons inside a parton jet).

When the main part of this work was carried out (Fall 1977) use in large $-p_T$ hadron production of parton distributions (including their Q^2 -dependence) obtained from lepton production analyses was justified only on probabilistic grounds (see Sect. 2.1, in particular Eq. (2.3)); no field-theoretic justification was available. It is now known that perturbative QCD fully justifies our approach. In particular Sachrajda^{(52), (53)} has considered the quark-gluon graphs corresponding to gluon radiative and vertex corrections to quark-quark scattering. To the order α_s^3 in the cross-section and in the leading logarithm approximation he has shown that these graphs, introduce scale violations in the parton distribution and fragmentation functions; and moreover, that to the same order in α_s , these scale violations are identical to those found in electroproduction by renormalization group and light cone techniques f_2 . The same result has been previously obtained by Politzer⁽⁵⁴⁾ in the Drell-Yan approach⁽⁵⁵⁾ to lepton-pair production and further extended by Sachrajda⁽⁵⁶⁾. Subsequent work has made clear that, in the leading logarithm approximation, these results hold to all orders of α_s ⁽⁵⁷⁾⁻⁽⁶¹⁾.

In Chapter II we present the general formalism of our work on $pp \rightarrow \pi^0 + X$ and $pp \rightarrow \frac{1}{2}(\pi^+ + \pi^-) + X$. In Chapter III we discuss the results of the calculations and compare with experiment. In Chapter IV we summarize our conclusions; we also discuss the main results on two-particle correlations. Moreover we examine possible connections of our approach with the CIM. Appendix A contains details on the parton distribution and fragmentation functions used in our calculations. Finally in Appendix B we discuss the sensitivity of our results to certain assumed inputs.

CHAPTER II

LARGE p_T SINGLE HADRON INCLUSIVE PRODUCTION

GENERAL FORMULATION

In this chapter and the next we present our work⁽⁶²⁾ on large p_T single hadron production. In the sense of perturbative QCD (Sec. 1.8) this is an application of now established formulas in the leading $\log Q^2$ approximation. Later (Sec. 4.3) we briefly consider possible effects of non-leading terms (corrections). We also incorporate the intrinsic transverse momenta of partons (hadrons) relative to their parent hadrons (partons).

2.1 The Inclusive Cross-Section with QCD and k_T Effects

The form of the invariant inclusive cross-section for $A+B \rightarrow C+X$ with parton (and hadron) intrinsic transverse momenta has already been considered in the framework of the naive parton model (without scale breaking)⁽⁶³⁾:

$$E_C \frac{d\sigma}{d^3p_C} (p_T, \theta, s) = \sum_{a,b,c} \int d^2 k_{Ta} \int d^2 k_{Tb} \int d^2 k_{Tc} \int dx_a \int dx_b f_{a/A} (x_a, \vec{k}_{Ta}) f_{b/B} (x_b, \vec{k}_{Tb}) \frac{1}{\pi} \frac{d\hat{\sigma}}{d\hat{t}} (\hat{s}, \hat{t}, \hat{u}) \frac{1}{z} G_{C/C} (z, \vec{k}_{Tc}) \quad (2.1)$$

Eq. (2.1) is a generalization of (1.10) (BBK model). In (2.1) $\frac{d\hat{\sigma}}{d\hat{t}}$ represents the differential cross-section for any subprocess $a+b \rightarrow c+d$ via which $A+B \rightarrow C+X$ is assumed to take place.

We shall use the same form for the hadronic cross-section, but:

- a) replace the scaling distribution and fragmentation functions by non-scaling ones; b) add the contributions of all the possible QCD scattering subprocesses with $\frac{d\sigma}{dt}$ calculated in the lowest order of perturbation theory and c) introduce the QCD running coupling constant. In this way we take into account the leading log effects to all orders of perturbation.

Thus we obtain the equation:

$$E_C \frac{d\sigma}{d^3 P_C} (p_T, \theta, s) = \sum_{a,b,c} \int d^2 k_{Ta} \int d^2 k_{Tb} \int d^2 k_{Tc} \int dx_a \int dx_b f_{a/A} (x_a, \vec{k}_{Ta}, Q^2) f_{b/B} (x_b, \vec{k}_{Tb}, Q^2) \frac{1}{\pi} \frac{d\hat{\sigma}}{d\hat{t}} (\hat{s}, \hat{t}, \hat{u}) \frac{1}{z} G_{C/c} (z, \vec{k}_{Tc}, Q^2) \quad (2.2)$$

where a,b,c represent quark (q), antiquark (\bar{q}) or gluon (g), $\hat{s}, \hat{t}, \hat{u}$ are the invariants of the subprocess and the variable Q^2 will be specified later.

The non-scaling parton distribution functions $f(x, \vec{k}_T, Q^2)$ are defined in the language of parton model by:

$$dP = f_{a/A} (x_a, \vec{k}_{Ta}, Q^2) dx_a d^2 k_{Ta} \quad (2.3)$$

where dP is the differential probability that a hadron A of momentum \vec{P}_A is seen by a probe of 4-momentum Q, to contain a parton a with longitudinal momentum $x_a \vec{P}_A$ and transverse momentum \vec{k}_{Ta} relative to \vec{P}_A . Correspondingly, the non-scaling parton fragmentation function $G(z, \vec{k}_{Tc}, Q^2)$ is defined by:

$$dP = \frac{1}{Z} G_{C/C} (z, \vec{k}_{TC}, Q^2) dz d^2 k_{TC} \quad (2.4)$$

where dP is the differential probability that a parton c of momentum \vec{p}_c is seen by a probe of 4-momentum Q , to produce a hadron C with longitudinal momentum $\vec{z}p_c$ and transverse momentum \vec{k}_{TC} relative to \vec{p}_c .

The summation over a, b, c in (2.2) stands for all possible lowest order subprocesses $ab \rightarrow cd$. For these subprocesses the corresponding differential cross-section $\frac{d\hat{\sigma}}{dt}$ is of the form:

$$\frac{d\hat{\sigma}}{dt} (ab \rightarrow cd) = \frac{\pi\alpha_s^2}{s} \sum_{ab \rightarrow cd} \quad (2.5)$$

The exact form of $\sum_{ab \rightarrow cd}$ for the various combinations $ab \rightarrow cd$ (Fig. 3) has been calculated in Refs. 47-49 and is given in Table 1. We have evaluated the contributions from all the subprocesses of this table in the case $\theta = 90^\circ$, $k_{Ti} = 0$, $i = a, b, c$ and we found that only the following cases give nonnegligible contributions

$$q_i q_j \rightarrow q_i q_j, \quad q_i g \rightarrow q_i g, \quad gg \rightarrow gg \quad (2.6)$$

where i and j denote quark flavors. In the multiple integral (2.2) we considered only the contributions from (2.6).

In (2.5), $\alpha = \alpha_s(Q^2)$ is the QCD running coupling (or fine structure) constant with the typical value (corresponding to four flavors)

$$\alpha_s(Q^2) = \frac{12\pi}{25 \log(Q^2/\Lambda^2)} \quad (2.7)$$

The invariants $\hat{s}, \hat{t}, \hat{u}$ are expressed in terms of the momentum fraction z and the integration variables $x_i, \vec{k}_{\tau i}$ ($i = a, b$) and $\vec{k}_{\tau c}$ by:^{f3}

$$\hat{s} = 2m_{\tau a} m_{\tau b} \left[\cosh (y_a - y_b) - \epsilon_{ab} \right] + 2m^2 \quad (2.8)$$

$$\hat{t} = -\frac{t}{z} + m^2 \quad (2.9)$$

$$\hat{u} = -\frac{u}{z} + m^2 \quad (2.10)$$

$$t_1 = 2m_{\tau a} m_{\tau c} \left[\cosh (y_a - y_c) - \epsilon_{ac} \right] \quad (2.11)$$

$$u_1 = 2m_{\tau b} m_{\tau c} \left[\cosh (y_b - y_c) - \epsilon_{bc} \right] \quad (2.12)$$

where

$$m_{\tau i}^2 = k_{\tau i}^2 + m^2 \quad i = a, b \quad (2.13)$$

$$m_{\tau c} = p'_\tau \quad \vec{p}' = \vec{p}_c - \vec{k}_{\tau c} \quad (2.14)$$

$$\epsilon_{ab} = \vec{k}_{\tau a} \cdot \vec{k}_{\tau b} / m_{\tau a} m_{\tau b} \quad (2.15)$$

$$\epsilon_{ic} = \vec{k}_{\tau i} \cdot \vec{p}' / m_{\tau i} m_{\tau c} \quad i = a, b \quad (2.16)$$

and the rapidities $y_{a,b,c}$ are given by:

$$\sinh y_a = \frac{x_a \sqrt{s}}{2m_{\tau a}} \quad (2.17)$$

$$\sinh y_b = \frac{x_b \sqrt{s}}{2m_{\tau b}} \quad (2.18)$$

$$\sinh y_c = \frac{p'_z}{m_{\tau c}} \quad (2.19)$$

In the above formulas m is the parton mass; we have taken

$$m_a = m_b = m = 300 \text{ MeV}, \quad m_c = m_d = 0 \quad (2.20)$$

irrespective of the flavor of a, b, c, d . A non-zero mass for c, d is unnecessary because the results are not sensitive to it while the formalism becomes complicated; it is however necessary for a, b because if $m = 0$ (2.13) gives $m_{\tau i} = 0$ when $k_{\tau i} = 0$ and leads to divergencies in (2.17) and (2.18). For this reason we also use the same value of m even when a or b is a gluon.

The constraint

$$\hat{s} + \hat{t} + \hat{u} = 2m^2 \quad (2.21)$$

together with the relations (2.9) and (2.10) determines the momentum fraction z in terms of integration variables:

$$z = \frac{u_1 + t_1}{\hat{s}} \quad (2.22)$$

In this way the invariants $\hat{s}, \hat{t}, \hat{u}$ in (2.8) - (2.10) contain only integration variables. The boundary of the integration region corresponds

to the limit $z = 1$; then (2.22) reduces to a quadratic equation for e^{y_a} in terms of the remaining variables:

$$A e^{2y_a} + B e^{y_a} + C = 0 \quad (2.23)$$

$$A = e^{-y_b} - \lambda_2 e^{-y_c} \quad (2.24a)$$

$$B = 2\lambda_3 - \lambda_1 (e^{y_b - y_c} + e^{y_c - y_b}) \quad (2.24b)$$

$$C = e^{y_b} - \lambda_2 e^{y_c} \quad (2.24c)$$

where

$$\lambda_1 = \frac{p_\tau}{m_{\tau a}}, \quad \lambda_2 = \frac{p_\tau}{m_{\tau b}}$$

$$\lambda_3 = \lambda_1 \epsilon_{bc} + \lambda_2 \epsilon_{ac} - \epsilon_{ab} + \frac{m^2}{m_{\tau a} m_{\tau b}} \quad (2.25)$$

The \vec{k}_τ dependence of the distribution functions $f(x, \vec{k}_\tau, Q^2)$ is generally unknown. We set

$$f(x, \vec{k}_\tau, Q^2) = \frac{F(x, \vec{k}_\tau, Q^2)}{x} \quad (2.26)$$

and proceed with the usual and convenient for calculations factorized Ansatz^{(41)-(43), (64)}

$$F(x, \vec{k}_\tau, Q^2) = F(x, Q^2) D(\vec{k}_\tau) \quad (2.27)$$

subject to

$$\int d^2 k_\tau D(\vec{k}_\tau) = 1 \quad (2.28)$$

Then, because of the resulting relation:

$$\int d^2 k_\tau F(x, \vec{k}_\tau, Q^2) = F(x, Q^2) \quad (2.29)$$

we may interpret $F(x, Q^2)$ as the longitudinal momentum distributions of partons in electroproduction. For $x = 0$, however, certain of the functions $F(x, Q^2)$ do not vanish; for $k_\tau \neq 0$ the point $x = 0$ is kinematically accessible, and this causes (2.26) and (2.2) to diverge. To avoid this, we introduce the modification (or redefinition) of $F(x, \vec{k}_\tau, Q^2)$ ^{(42), (43)}

$$f(x, \vec{k}_\tau, Q) = \frac{F(x, \vec{k}_\tau, Q^2)}{x_R} \quad (2.30)$$

where x_R is the energy fraction carried by the parton

$$x_R = \left(x^2 + \frac{4m_\tau^2}{s} \right)^{1/2}, \quad m_\tau^2 = k_\tau^2 + m^2 \quad (2.31)$$

and the function $F(x, \vec{k}_\tau, Q^2)$ in (2.30) is given by the factorized form (2.27). In the absence of any information we use the Ansatz (2.27) for all partons (quarks, antiquarks and gluons), as well as for the fragmentation functions.

$$G_{C/C}(z, \vec{k}_{\tau C}, Q^2) = G_{C/C}(z, Q^2) D(\vec{k}_{\tau C}) \quad (2.32)$$

In the presence of parton k_T the kinematical invariants \hat{s} , \hat{t} and \hat{u} may become very small and cause (2.5) and the expressions of $\Sigma_{ab \rightarrow cd}$ (Table 1) to diverge. To avoid this we make the replacements^{(41),(42)}:

$$\hat{s} \rightarrow \hat{s} + M^2, \quad \hat{t} \rightarrow \hat{t} - M^2, \quad \hat{u} \rightarrow \hat{u} - M^2 \quad (2.33)$$

with the typical hadronic mass scale $M = 1$ GeV. We have checked that at sufficiently large p_T (> 3 GeV) the predictions are not sensitive to the precise value of M (see Appendix B for details).

The evaluation of the multifold integral in (2.2) has been carried out with Monte Carlo techniques. Details of the integration procedure are presented in Appendix A of our publication, Ref. 62.

2.2 Distribution and Fragmentation Functions from QCD

We are interested in hadron production in proton-proton collisions ($A = B = P$). Then using the notation:

$$xf_{a/p}(x, Q^2) = F_{a/p}(x, Q^2) = a, \quad a = u, d, s, \bar{u}, \bar{d}, \bar{s} \quad (2.34)$$

we write

$$u = u_v(x, Q^2) + t(x, Q^2) \quad (2.35)$$

$$d = d_v(x, Q^2) + t(x, Q^2) \quad (2.36)$$

$$s = \bar{s} = \bar{u} = \bar{d} = t(x, Q^2) \quad (2.37)$$

where $u_v(x, Q^2)$, $d_v(x, Q^2)$ and $t(x, Q^2)$ are the momentum distributions of u-valence, d-valence and sea quarks inside the proton and an SU(3)-symmetric sea has been assumed. Similarly when a is a gluon we set:

$$xf_{g/p}(x, Q^2) = F_{g/p}(x, Q^2) = g(x, Q^2) \quad (2.38)$$

The explicit form of the distributions u_v , d_v , t and g as functions of x and Q^2 has been obtained from Ref. 51 which makes a detailed account of the QCD requirements and fits the available data on nucleon structure functions^{(50), (51)}. The Q^2 dependence of these distributions is specified by the QCD variable

$$\tilde{s} = \log \frac{\log(Q^2/\Lambda^2)}{\log(Q_0^2/\Lambda^2)} \quad (2.39)$$

with

$$Q_0^2 = 1.8 \text{ GeV}^2, \quad \Lambda = 0.3 \text{ GeV} \quad (2.40)$$

We present all these functions in detail in Appendix A.

To determine the non-scaling form of the quark fragmentation functions we are guided by the QCD solutions of Gross⁽⁷¹⁾ and Politzer^(26a), which have also been used in other similar calculations^{(30), (49)} f_i . The fact that these solutions are valid for z not very small does not affect the predictions because most of the contribution to (2.2) comes from the region near $z \sim 1$. Thus we take^{f5}:

$$G_{C/c}(z, \bar{s}) = g_{C/c} e^{A\bar{s}} \frac{(1 + m_{C/c}(0))}{(1 + m_{C/c}(\bar{s}))} (1-z)^{m_{C/c}(\bar{s})} \quad (2.41)$$

where the variable \bar{s} carrying the Q^2 dependence is given again by (2.39) with the same values of the parameters Λ and Q_0^2 ; $g_{C/c}$ are constants and

$$m_{C/c}(\bar{s}) = m_{C/c}(0) + 4G\bar{s} \quad (2.42)$$

where the standard QCD model of four flavors and three colors gives⁽⁷¹⁾:

$$G = \frac{4}{25}, \quad A = 0.69 G \quad (2.43)$$

The functions $G_{C/c}$ are subject to the momentum conservation sum rule:

$$\sum_C \int_0^1 G_{C/c}(z, \bar{s}) dz = 1 \quad (2.44)$$

for every species c .

For $\bar{s} = 0$ ($Q^2 = Q_0^2$) we obtain from (2.41) and (2.42) the corresponding scaling forms

$$G_{C/c}(z) = g_{C/c} (1-z)^{m_{C/c}(0)} \quad (2.45)$$

$$\sum_C \int_0^1 G_{C/c}(z) dz = \sum_C \frac{g_{C/c}}{1 + m_{C/c}(0)} = 1 \quad (2.46)$$

The values of $m_{C/c}(0)$ are determined from an analysis of hadron electroproduction data and the values of $g_{C/c}$ from the same analysis and the sum rule (2.46). All of them are given in Appendix A.

We should note that for the non-scaling form (2.41) and with $g_{C/c} = \text{constants}$, the sum rule (2.44) cannot be satisfied for all \bar{s} . Therefore we are contented to satisfy (2.44) exactly for $\bar{s} = 0$ [Eq. (2.46)] and notice that, owing to the weak dependence of \bar{s} on Q^2 [Eq. (2.39)] the violation is $\lesssim 10\%$ for all Q^2 of interest.

As we mention in Sec. 1.8, perturbative QCD predicts scaling violations for (all) the fragmentation functions^{(52), (60)}. Data on electroproduction of pions⁽⁷²⁾, however, appear to be compatible with scaling ones. In order to study in more detail the sensitivity of the cross-section (2.2) on the scaling violations of $G_{C/c}$ we present complete calculations both with scaling and non-scaling quark fragmentation functions and discuss the comparison between theory and experiment in Sec. 3.2.

For the gluon fragmentation function we take for simplicity a scaling form:

$$G_{C/g} = g_{C/g} (1-z)^{m_{C/g}} \quad (2.47)$$

subject to a sum rule such as (2.46):

$$\sum_C \frac{g_{C/g}}{1 + m_{C/g}} = 1 \quad (2.48)$$

The effect of non-scaling $G_{C/g}$ is discussed in Sec. 4.2.

CHAPTER III

CALCULATIONS AND COMPARISON WITH EXPERIMENT

In this chapter we present some details of our calculations together with our main conclusions concerning the effects of intrinsic transverse momentum. Also we present our basic results and compare them with experimental data.

3.1 Calculations and Conclusions on k_T Effects

The form of the intrinsic transverse momentum distributions $D(k_T)$ [Eqs (2.27), (2.32)] of partons (hadrons) relative to their parent hadrons (partons) is not known theoretically. We have carried calculations by choosing simple (and physically reasonable) distributions of exponential and Gaussian form; we present detailed results for the former case and discuss in Appendix B the (not much different) effects of the latter.

For any type of parton we put in (2.27) and (2.32):

$$D(\vec{k}_T) = \frac{b^2}{2\pi} \exp(-bk_T) \quad (3.1)$$

which has been normalized to satisfy (2.28). The parameter b is related to the average value of k_T by:

$$\langle k_T \rangle \equiv \int d^2 k_T k_T D(\vec{k}_T) = \frac{2}{b} \quad (3.2)$$

It is generally believed that $\langle k_T \rangle$ is Q^2 independent and of the order of a few hundred MeV. For simplicity we do not investigate a possible

x-dependence of $\langle k_T \rangle$ and choose the constant value:

$$\langle k_T \rangle = 0.5 \text{ GeV} \quad (b = 4 \text{ GeV}^{-1}) \quad (3.3)$$

This value is consistent with the results of various analyses⁽⁷⁶⁾⁻⁽⁷⁸⁾ of the transverse momentum (q_T) distributions of massive muon pairs produced in pp collisions. In these analyses the q_T distribution is calculated by taking into account: a) the perturbative contribution^{(54),(79)-(81)} due to the recoiling gluon (quark) in the subprocess $q\bar{q} \rightarrow \gamma^* + q$ ($qg \rightarrow \gamma^* + q$) in which the virtual photon γ^* decays into a $\mu^+\mu^-$ pair, b) the non-perturbative contribution due to the intrinsic k_T of the initial partons. These two contributions are properly combined according to a regularization prescription proposed in Ref. 76, and an overall good fit to the data is obtained with a value of intrinsic $\langle k_T \rangle = 0.5 \sim 0.6 \text{ GeV}$ ⁽⁷⁶⁾⁻⁽⁷⁸⁾.

To show clearly our results on the k_T effects of quarks and gluons we have separated in Fig. 4 the contributions of the subprocesses qq , qg and gg , for $\sqrt{s} = 52.7 \text{ GeV}$. All results of Fig. 4 correspond to scaling fragmentation functions $G_{C/c} = G_{C/c}(z)$ and an input gluon distribution (see Appendix A),

$$g(x, Q_0^2) = .402 (\gamma + 1) (1-x)^\gamma \quad (3.4)$$

with $\gamma = 5$. With the same choice as above we present in Fig. 5 the total cross-section for two different energies $\sqrt{s} = 52.7$ and 19.4 GeV . Our conclusions can be summarized as follows:

- (a) At fixed s , as p_T increases the k_T effects always decrease. E.g., at $\sqrt{s} = 52.7$ the k_T effects increase the qq contribution by a

factor of ~ 2 at $p_T = 2$ GeV, but only by ~ 1.1 at $p_T = 8$ GeV (Fig. 4). These are typical results of other similar calculations^{(41)-(43),(73)} as well. The decrease of the k_T effects is intuitively clear^{(44),(74),(75)} (see Sec. 1.7).

- (b) At fixed p_T , as s decreases, the k_T effects increase (Fig. 5). E.g., at $\sqrt{s} = 19.4$ and $p_T = 2$ GeV they increase the qq contribution by a factor of ~ 3 . This aspect has also been observed^{(42),(43)}.
- (c) The transverse momentum of the gluon has a very important effect (at intermediate p_T). E.g., at $\sqrt{s} = 52.7$ and $p_T = 2$ GeV it enhances the qq contribution by a factor of ~ 2.6 and the gg contribution by ~ 5 (to be compared with the factor ~ 2 for the qq contribution). Qualitatively this is understood as follows: In general, the stronger the p_T dependence of a given contribution is, the stronger (percentagewise) the k_T effects are (Sec. 1.7). The qq and in particular the gg contribution has a very strong p_T dependence (Fig. 4); this is due to the exponent of $1-x$ of $g(x, Q^2)$, which is already large at $Q^2 = Q_0^2$ but increases relatively fast with $Q^2 \sim p_T^2$ (see Appendix A). This results in stronger k_T effects.
- (d) The transverse momentum \vec{k}_{TC} of the hadron C relative to the parton c (\vec{k}_{TC} dependence of the fragmentation function) has a small effect in the single particle inclusive cross-section. (It has, however, a large effect in the two particle inclusive cross-section⁽⁸²⁾).

All the above conclusions remain qualitatively the same for non-scaling fragmentation functions or for different values of the exponent γ in (3.4) (see next Section).

3.2 Comparison with Experiment

The predicted inclusive cross-sections for $pp \rightarrow \pi^0 + X$ (and $pp \rightarrow \frac{1}{2}(\pi^+ + \pi^-) + X$) are presented and compared with data in Fig. 5. (scaling $G_{C/C}$) and Fig. 6 (non-scaling quark $G_{C/C}$). In both cases the exponent γ in the input gluon [Eq. (3.4)] has been taken $\gamma = 5$.

We see that inclusion of intrinsic k_T effects accounts fairly well for the magnitude and the p_T dependence of the ISR data, down to $p_T \approx 2$ GeV. The predictions are in good agreement with the very large p_T (≥ 7 GeV) data ⁽⁸³⁾. This is certainly true for scaling $G_{C/C}$. As one expects, inclusion of scale violations in the quark fragmentation functions somewhat increases the p_T dependence and lowers the predictions (Fig. 6).

We should note, however, that recent (Fall 1978) very large p_T ($7 \lesssim p_T \lesssim 12$) data ⁽⁸⁴⁾ are somewhat below those of Ref. 83. Then the predictions with scale violations in the fragmentation functions are in better agreement, in favor of the QCD results, requiring non-scaling fragmentation functions. We discuss this point further in Sec. 4.2.

The p_T dependence of the Fermilab data ($\sqrt{s} = 19.4$) is also predicted reasonably well (in particular, Fig. 5); however, the predicted cross-sections lie somewhat below the experimental ones. The difficulty to account for the correct energy dependence at fixed p_T has also been observed in other applications of the scale violating approach. ^{(30), (32), (47)} However possible corrections can be invoked, which we discuss in Sec. 4.3.

A very important rôle in the energy dependence is played by the exact shape of the gluon distribution at $Q = Q_0$ (the exponent γ in (3.4)). Decreasing γ , weakens the x_T dependence and thus enhances the qg and gg contributions particularly at Fermilab energies (larger $x_T = \frac{2p_T}{\sqrt{s}}$).

To show this effect we present in Fig. 7 calculations for $\gamma = 3$ and 10. For $\gamma = 3$ with the inclusion of partons' k_T the predictions are almost the same for ISR data, but in somewhat better agreement (than for $\gamma = 5$, Fig. 5) with Fermilab data, in particular at $p_T = 2$ GeV.

The shape of the gluon distribution at $Q = Q_0$ is to a great extent unknown. Values in the range $3 \leq \gamma \leq 10$ have been suggested⁽⁸⁵⁾ and considered in other QCD applications^{(50), (51), (86)}. The aforementioned sensitivity to the energy dependence is rather weak and does not lead to a specific value. In most of our calculations we use $\gamma = 5$ in accord with naive counting rules⁽⁸⁷⁾.

CHAPTER IV

DISCUSSION AND CONCLUSIONS

4.1 Summary of Our Work

In this work we have studied the inclusive meson production at large p_T in hadronic collisions, making explicit calculations for the typical process $pp \rightarrow \pi^0 + X$ (and $pp \rightarrow \frac{1}{2} (\pi^+ + \pi^-) + X$).

Our general framework was the QCD improved parton model, which can be applied to all (high energy) processes involving hadrons in the initial and/or final states. This framework inter-relates the various processes by permitting the information gained from some of them to be used in more complex ones. Therefore, it is possible to make predictions for the latter processes and thus test the theory (QCD) by comparing with available experimental data.

We used a) the quark distribution functions obtained from lepton initiated processes $ep \rightarrow e + X$, $\mu p \rightarrow \mu + X$ and neutrino and antineutrino interactions, and b) the quark fragmentation functions obtained from hadron production in $e^+ e^-$ annihilation and from the semi-inclusive processes $ep \rightarrow e + h + X$ and $\nu p \rightarrow \mu^- + h + X$; then we performed explicit calculations for the purely hadronic process $pp \rightarrow \pi^0 + X$ "explaining" the data and testing the theory (Fig. 5-7).

The unknowns in our calculations were the power γ [Eq. (3.4)] determining the shape of the gluon distribution function, the corresponding power for the gluon fragmentation, and to some extent the average value of the intrinsic parton transverse momentum. We did not try to obtain an optimal fit to the data by adjusting these unknowns. In particular

the absolute magnitude of $E \, d\sigma/dp^3$ is specified from the magnitude of the running coupling constant $\alpha_s(Q^2)$.

We find that we essentially account for the main features of the data, and we may conclude that QCD accounts for large p_T single meson production reasonably well, certainly at ISR energies.

4.2 Main Results from Large-Transverse Momentum Correlations

After the completion of the main part of this thesis⁽⁶²⁾, the preceding QCD approach was also applied to large- p_T two hadron inclusive reactions and correlations at ISR energies⁽⁸²⁾. In particular we studied opposite side hadron correlations, which are known to be particularly sensitive to details of the dynamics⁽⁸⁸⁾,^(19b),⁽³³⁾.

For pp collisions we calculated and compared with data the following quantities:

- (a) Normalized transverse momentum sharing (x_e) distributions $\frac{1}{N} \frac{dN}{dx_e}$, vs trigger momentum p_{T1} , for several bins of $x_e \equiv \frac{p_{x2}}{p_{T1}}$.
- (b) Normalized x_e -distributions $\frac{1}{N} \frac{dN}{dx_e}$, vs x_e , for different trigger momentum p_{T1} .
- (c) Integrated x_e -distributions $\frac{1}{N} \int_{x_{e-\min}}^{\infty} \frac{dN}{dx_e} dx_e$, vs trigger p_{T1} , for $x_{e-\min} = 0.5$ and $1..$
- (d) Rapidity distributions $\frac{1}{N} \frac{dN}{dy_2 d\phi_2}$, vs the (pseudo-) rapidity y_2 of the secondary.

Our calculations⁽⁸²⁾ indicate that scale violations in all the fragmentation functions are important in obtaining agreement with experiment for all the above quantities (a)-(d).

On the other hand, scale violations in $G_{\pi/g}$ will affect the single particle cross-section [Eq. (2.2)] to a limited extent. For $p_T \geq 5$ GeV

the dominant contribution comes from qq scattering (see Fig. 4) so that the exact form of $G_{\pi/g}$ is not very important. At $p_T \approx 2-5$ GeV, the predicted $E \frac{d\sigma}{d^3p}$ will be somewhat smaller. However, as we discuss below, in this region of p_T other contributions may be important.

4.3 Possible Corrections

The fact that QCD predictions are somehow below the data at $p_T \approx 2-5$ GeV and/or at FNAL energies can probably be explained by invoking the following corrections:

(a) Uncertainties in some parameters.

At low p_T the results are sensitive to: (α_1) the precise input gluon distribution; decreasing γ increases the cross-section (Fig. 7) and improves the agreement with experiment. (α_2) the value of the momentum scale Λ ($\Lambda = 0.3-0.6$ GeV). In our calculations we used $\Lambda = 0.3$ GeV, but perhaps higher values of Λ are preferable. Increasing Λ , increases the predictions at low p_T (with $\Lambda = 0.6$ GeV $E \frac{d\sigma}{d^3p}$ is higher by a factor of 2 at $p_T = 2$ GeV and $\sqrt{s} = 53$ GeV than that with $\Lambda = 0.4$ GeV⁽⁸⁹⁾). (α_3) the precise choice of Q^2 (see Appendix B).

(b) Nonleading corrections from higher order diagrams.

At small Q^2 (small p_T) the nonleading terms of the higher order QCD subprocesses, as $qq \rightarrow qqg$ and more generally of the $2 \rightarrow 3$ or $2 \rightarrow n$ Feynman graphs, may contribute. It is now clear^{(52), (57)-(61)} that only the leading $\log Q^2$ pieces of those graphs are included in the renormalization group improved distribution or fragmentation functions. At present, however, there exists no calculation of the nonleading terms for large- p_T hadron production.

(c) Larger value of $\langle k_T \rangle$.

A somewhat larger value of $\langle k_T \rangle$ (~ 0.6 GeV) is also consistent with the analyses⁽⁷⁶⁾⁻⁽⁷⁸⁾ of transverse momentum (q_T) distributions of massive muon pairs produced in pp collisions (See Sec. 3.1). Larger $\langle k_T \rangle$ will increase the inclusive cross-section at small p_T , especially at FNAL energies, where the p_T dependence is stronger (Figs. 5-7), and will improve the agreement with experiment.

In fact, Field with $\langle k_T \rangle = .848$ GeV obtained good fits to the data at both energies $\sqrt{s} = 53$ and 19.4 GeV⁽⁹⁰⁾; subsequently other authors verified this conclusion^{(91),(92)}. Such a very large value of $\langle k_T \rangle$ has been interpreted as effective value representing both the intrinsic transverse momentum of the partons and the transverse momentum due to the Bremsstrahlung of gluons. This point of view, however, is questionable^{(93),(94)}. Also notice that with such values of $\langle k_T \rangle$ the inclusive cross-section is very sensitive to the cutoff required at low \hat{s}, \hat{t} and \hat{u} . [see relations (2.33)].

(d) CIM Contributions.

In addition to the parton-parton scattering, CIM subprocesses can be considered, as in section 1.4, Eqs. (1.15). Recently, Blankenbecler, Brodsky and Gunion⁽⁹⁵⁾ were able to determine the normalization of the subprocesses and the probability density of finding a meson inside a hadron especially $F_{\pi/p}(x)$. Thus the CIM has been cured from that disease and is capable of making definite predictions. Calculations⁽⁹⁵⁾⁻⁽⁹⁷⁾ indicate that the CIM terms are important at the low p_T region, with the leading QCD subprocesses (parton-parton scattering) dominating for $p_T \gtrsim 5$ GeV.

Qualitatively this can be understood as follows: In any quark or gluon scattering subprocess there is a numerical suppression of the

inclusive cross-section, because of the rapidly falling fragmentation function $G_{\pi/g}(z, Q^2)$ or $G_{\pi/g}(z, Q^2)$ at $z \rightarrow 1$. On the other hand, if the pion trigger emerges directly from the subprocess (as in the CIM $Mq \rightarrow \pi q$) there is no suppression due to fragmentation. Furthermore, due to the rapid falloff of the CIM cross-section with p_τ ,

$$\frac{d\hat{\sigma}}{dt}(qM \rightarrow qM) = \frac{\pi\alpha_m^2}{s u} \sim \frac{1}{p_\tau^8} \quad (4.1)$$

their contribution cannot be dominant at high p_τ .

Other arguments in favor of the CIM contributions at small p_τ are the following:⁽⁹⁴⁾

- i) The form (4.1) for $\frac{d\hat{\sigma}}{dt}$ is similar to that proposed in the 'Black-Box' model Eq. (1.18), giving the best fit to the angular distribution of $pp \rightarrow \pi + X$.
- ii) The CIM mechanism predicts that the trigger particle usually emerges alone, without same side correlated particles. This seems to be in agreement with the BFS⁽⁹⁸⁾ experiment at ISR with a 4 GeV trigger (in $\sim 85\%$ of the events the trigger particle is unaccompanied by same side charged particles).
- iii) The $qM \rightarrow qM'$ subprocess implies that flavor is generally exchanged in the hard scattering reaction. Thus the charge and flavor of the away side jet in the CIM can be correlated with the flavor quantum numbers of the trigger. In contrast, the QCD diagrams predict very small⁽⁸⁹⁾ flavor correlations between the away-side and same-side systems. The data from the BSF-ISR collaboration show striking flavor correlations in agreement with CIM.

iv) In the case of $pp \rightarrow p + X$, the dominant CIM subprocess is $q\bar{q} \rightarrow q\bar{q}$, leading to a behaviour of the inclusive cross-section (at fixed x_T and θ_{cm}) $E \frac{d\sigma}{d^3p} \sim \frac{1}{p_T^2}$, in agreement with the Chicago-Princeton⁽⁹⁹⁾ data at FNAL τ energies and $p_T < 7$ GeV. On the other hand, there seems no way to account for the p_T -dependence of $pp \rightarrow p + X$ in terms of QCD subprocesses (without enormous scale-breaking in the fragmentation functions of partons to protons). If CIM contributions are dominant in baryon production they may also be present in meson production.

Thus there is much evidence that the CIM contribution provide important corrections to the QCD subprocesses at the small p_T region in inclusive meson production.

4.4 Overall Conclusions

Our conclusions can be summarized as follows:

QCD predictions for inclusive pion production at large transverse momenta in pp collisions are in good agreement with experiment, at least for ISR energies and $p_T \gtrsim 5$ GeV. Also for ISR energies data on two-particle opposite-side correlations are reasonably well accounted for.

The intrinsic transverse momenta (k_T) of partons inside their parent hadrons are important for the single particle cross-section in the small p_T region; they increase the cross-section by at least a factor of 2 at $p_T \approx 2$ GeV. Also the intrinsic transverse momenta of hadrons with respect to the parent partons are important for the two particle inclusive cross-section^{(33), (88), (100)}.

The fact that the predicted cross-section for $pp \rightarrow \pi + X$ lies somewhat below experiment at Fermilab energies and for the small p_T region

at ISR energies, cannot be considered as a serious trouble of QCD. At relatively low energies and/or p_T , (small Q^2) many subasymptotic effects take place. Probably the most important of these are the CIM subprocesses (called also "higher twist" - QCD⁽⁹⁴⁾).

APPENDIX A

DETAILS ON DISTRIBUTION AND FRAGMENTATION FUNCTIONS

In this Appendix we present the detailed forms of the parton distribution and fragmentation functions used in the calculations.

A 1. Distribution Functions.

Throughout the work we used the distributions of Ref. 51. With the definitions (2.34) and (2.38) and decompositions (2.35)-(2.37) the formalism of Ref. 51 leads to the expressions presented below.

The valence distributions are:

$$u_v = \frac{3}{B(\eta_1, 1+\eta_2)} x^{\eta_1} (1-x)^{\eta_2} - d_v \quad (A 1)$$

$$d_v = \frac{1}{B(\eta_3, 1+\eta_4)} x^{\eta_3} (1-x)^{\eta_4} \quad (A 2)$$

with

$$\eta_i = \eta_i(\bar{s}) = \eta_i(0) + \gamma_i G\bar{s} \quad (i = 1, \dots, 4) \quad (A 3)$$

where $G = \frac{4}{25}$ (as in Eq. (2.43)) and,

$$\eta_1(0) = 0.7, \eta_2(0) = 2.6, \eta_3(0) = 0.85, \eta_4(0) = 3.35, \quad (A 4)$$

$$\gamma_1 = -1.1, \gamma_2 = 5.0, \gamma_3 = -1.5, \gamma_4 = 5.1. \quad (A 5)$$

In (A 1) and (A 2), $B(\eta_j, 1+\eta_{j+1})$ $j = 1, 3$ are Euler's beta functions.

The sea and gluon distributions are expressed as

$$t = \frac{1}{6} \frac{\tau_2}{\tau_3} (\tau_2 - \tau_3) (1-x)^{(\tau_2/\tau_3)-2} \quad (\text{A } 6)$$

$$g = \frac{G_2}{G_3} (G_2 - G_3) (1-x)^{(G_2/G_3)-2} \quad (\text{A } 7)$$

where all the above variables are \bar{s} dependent.

The exponent γ in Eq. (3.4) is connected with the above parametrization by:

$$\gamma = \frac{G_2(0)}{G_3(0)} - 2 \quad (\text{A } 8)$$

Variation of γ in the input gluon distribution at the reference momentum $Q^2 = Q_0^2$ ($\bar{s} = 0$) affects the sea and gluon distributions at other values of $Q^2 > Q_0^2$ ($\bar{s} > 0$). With the decomposition

$$\tau_j = \frac{1}{4} A_j + \frac{3}{4} B_j, \quad j = 2, 3 \quad (\text{A } 9)$$

the formalism of Ref. 51 leads to the following results

$$A_2 = 0.11 \exp (-0.427 \bar{s})$$

$$A_3 = 9.167 \times 10^{-3} \exp (-0.667 \bar{s})$$

$$B_2 = 0.429 + 0.169 \exp (-0.747 \bar{s}) - 0.488 \exp (-0.667 \bar{s})$$

$$B_3 = (1.246 \times 10^{-2} - \frac{0.11577}{\gamma + 2}) \exp (-1.386 \bar{s}) \quad (\text{A } 10)$$

$$+ (0.15376 + \frac{0.11577}{\gamma + 2}) \exp (-0.609 \bar{s}) - 0.157 \exp (-0.667 \bar{s})$$

$$G_2 = 0.571 - 0.619 \exp (-0.747 \bar{s})$$

$$G_3 = \left(\frac{3.015 \times 10^{-2}}{\gamma + 2} + 4.0027 \times 10^{-2} \right) \exp(-0.609 \bar{s}) \\ + \left(\frac{0.37185}{\gamma + 2} - 4.0027 \times 10^{-2} \right) \exp(-1.386 \bar{s})$$

where only B_3 and G_3 are γ dependent.

A 2. Parameters of Fragmentation Functions.

The parameters $m_{G/c}(0)$ and $g_{G/c}$ of the quark fragmentation functions, Eq. (2.41), are specified as follows: When c is a valence quark of π^\pm or K^\pm (e.g., u of π^+) we take

$$m_{\pi^\pm/c}(0) = m_{K^\pm/c}(0) = 1 \quad (A 11)$$

which is in accord with hadron leptonproduction analyses^{(44),(101)} as well as with counting rules⁽¹⁵⁾. When c' is a nonvalence quark of π^\pm or K^\pm (e.g., u of π^-) we take^{(49),(101)}

$$m_{\pi^\pm/c'} = m_{K^\pm/c'} = 1.5. \quad (A 12)$$

The same leptonproduction analyses require

$$g_{\pi^+/u} = 2g_{\pi^-/u} \quad (A 13)$$

and fits to $pp \rightarrow K^\pm + X$ require⁽³²⁾

$$g_{\pi^+/u} = 2g_{K^+/u} = 4g_{K^-/u} \quad (A 14)$$

Also, we take as usual

$$G_{\pi^0/c}(z, Q^2) = \frac{1}{2} \left[G_{\pi^+/c}(z, Q^2) + G_{\pi^-/c}(z, Q^2) \right] \quad (A 15)$$

Then, leaving out baryons⁽³²⁾, the sum rule (2.46) is satisfied by:

$$g_{\pi^+/u} \approx 0.75 \quad (A 16)$$

in fair agreement with Refs. 49, and 101.

For the gluon fragmentation function, Eq. (2.41), we also assume that the sum rule (2.48) is saturated by $C = \pi^\pm, \pi^0$ and K^\pm (no baryons). For all these mesons we take

$$m_{C/g} = 1, \quad C = \pi^\pm, \pi^0, K^\pm \quad (A 17)$$

this (or a similar) value is also used in other calculations⁽⁴⁷⁾⁻⁽⁴⁹⁾.

We take

$$g_{\pi^+/g} = g_{\pi^-/g} = g_{\pi^0/g}, \quad g_{K^+/g} = g_{K^-/g} \quad (A 18)$$

and

$$g_{\pi^+/g} = 2g_{K^+/g} \quad (A 19)$$

as suggested by the first of Eq. (A 14). Then the sum rule (2.48) implies

$$g_{\pi^+/g} \approx 0.5 \quad (A 20)$$

APPENDIX B

SENSITIVITY IN ASSUMED INPUTS

B 1. M-Dependence

In the presence of k_T effects, to avoid divergence of $\frac{d\hat{\sigma}}{dt}$ we made the replacements (see relations (2.33)),

$$\hat{s} \rightarrow \hat{s} + M^2, \quad \hat{t} \rightarrow \hat{t} - M^2, \quad \hat{u} \rightarrow \hat{u} - M^2$$

We tested the sensitivity of our predictions by varying M^2 in the range $0.09 < M^2 < 1$. With our value $\langle k_T \rangle = 0.5$ GeV we found that for $p_{T\gamma} > 3$ GeV the results are not sensitive. For $p_{T\gamma} = 2$ GeV the predicted $E \frac{d\hat{\sigma}}{d^3p}$ are enhanced by factors $\lesssim 2$ at ISR and by factors $\lesssim 4.5$ at FNAL energies.

The insensitivity of our results at $p_{T\gamma} > 3$ GeV is due to the relatively small value of our $\langle k_T \rangle$; for higher values the dependence on the cutoff M is stronger. We may say that the value $M = 1$ GeV of our calculations does not exaggerate the k_T effects.

Recently calculations based on off-shell constituent kinematics^{(93),(102),(103)} have been carried out⁽¹⁰⁴⁾. In this way the poles $\hat{s}, \hat{t}, \hat{u} = 0$ lie outside the allowed phase space boundary and there is no need of cutoff. The result of these calculations is that at ISR energies and $p_{T\gamma} = 2$ GeV the k_T effects increase the inclusive cross-section by a factor of ~ 2 . This is in good agreement with our result.

B 2. Scaling Variable

An important question is the choice of the scaling variable [Bjorken x , $x^{(105)}$ or $\xi^{(106)}$] that best accounts for mass effects (corrections of

$\sigma(\frac{1}{2})$). It is possible that such effects are still important at $\sqrt{s} = 19.4$ but they practically disappear at $\sqrt{s} = 52.7$ GeV. To investigate this question we have replaced in the gluon distribution the variable x by the Nachtmann variable

$$\xi = \frac{2x}{1 + (1 + 4x^2 M^2/Q^2)^{1/2}}$$

and have calculated, according to Appendix A and Ref. 51, the necessary changes in the sea distribution.

As expected, we found that at $\sqrt{s} = 19.4$ GeV this replacement somewhat improves the agreement and at $\sqrt{s} = 52.7$ GeV leaves our results unaffected. However, for $M = \text{nucleon mass}^{(106)}$ the change is very small.

B 3. Gaussian Distribution of k_T

We also carried calculations with a Gaussian form of the function $D(\vec{k}_T)$, [Eq. (2.27)].

$$D(\vec{k}_T) = \frac{b^2}{\pi} \exp(-b^2 k_T^2)$$

where we took again

$$\langle k_T \rangle = \frac{\pi}{2b} = 0.5 \text{ GeV};$$

As expected, the k_T effects were somewhat (but not much) smaller.

B 4. Choice of Q^2

A problem we have faced concerns the choice of the variable Q^2 in the functions $F_{a/A}(x, Q^2)$, $G_{C/C}(z, Q^2)$ and in the running coupling constant $\alpha_s(Q^2)$. In ep collisions, Q is the 4-momentum transfer from the electron to the quark (4-momentum of the virtual photon). On the other hand, for the subprocesses shown in Fig. 3 the choice of Q^2 is complicated by questions of gauge invariance^{(47), (49)}.

In our calculations we have always chosen Q to be the 4-momentum of the parton exchanged in the subprocess $ab \rightarrow cd$, irrespective of whether the exchange takes place in the \hat{t} , \hat{u} or \hat{s} channel.

We also carried calculations taking $Q^2 = -\hat{t}$; for hadron production at $\theta = 90^\circ$ this reduces to the previous choice only for $qq \rightarrow qq$ ($Q^2 = -\hat{t} = -\hat{u}$). The results were not significantly altered ($\lesssim 25\%$). Other similar calculations^{(47), (49)} with a variety of choices of Q^2 lead to the same conclusion.

The extension of our QCD approach to two-hadron correlations⁽⁸²⁾ shows that in general the choice of Q^2 somewhat affects the shape of the opposite-side rapidity distribution $(\frac{1}{N} \frac{dN}{dy d\phi})$ and the position of its peak. Details are discussed in our publication⁽⁸²⁾.

FOOTNOTES

- f1. If there is no incoming (observed outgoing) hadron in the process under consideration, the corresponding parton distribution (fragmentation) function, has to be replaced by a delta function.
- f2. See e.g. Ref. 53 for the justification of using the renormalization group improved distribution and fragmentation functions and the running coupling constant and all the parton-parton scattering subprocesses (qq, qg and gg)
- f3. We follow essentially the notation of Ref. 43.
- f4. Reciprocity relations⁽⁶⁵⁾ require that at least for $z \rightarrow 1$ $G_{C/c}$ behaves as $F_{A/A}$ for $x \rightarrow 1$; there are also other field-theoretic arguments⁽⁶⁶⁾ and model calculations⁽⁶⁷⁾ suggesting scale violations for $G_{C/c}$ similar to those of $F_{A/A}$. Recently it was demonstrated⁽⁶⁸⁾ that the scale violations in $G_{C/c}$ are determined by similar (transposed) integrodifferential matrix equations⁽⁶⁹⁾. Furthermore it can be seen that for $z \rightarrow 1$ these matrix equations decouple and the Q^2 dependence of the quark fragmentation function is the same as that of the valence quark distribution for $x \rightarrow 1$. This fully justifies our approach.
- f5. The solution of Ref. 71 involves $(-lnz)^{m_{G/c}(\bar{s})}$ instead of $(1-z)^{m_{G/c}(\bar{s})}$. For $z \rightarrow 1$, however, $-lnz \approx 1-z$.

TABLE 1

Cross sections for the various subprocesses $ab \rightarrow cd$ to lowest order in QCD. $\Sigma_{ab \rightarrow cd}$ is defined in Eq. (2.5). The initial (final) colours and spins have been averaged (summed). Subscripts i, j denote quark flavors. The original derivation is by Combridge, Kripfganz and Ranft, Ref. 47.

	$ab \rightarrow cd$	$\Sigma_{ab \rightarrow cd}$
1	$q_i q_j \rightarrow q_i q_j \quad (i \neq j)$	$\frac{4}{9} \frac{s^2 + u^2}{t^2}$
2	$q_i \bar{q}_j \rightarrow q_i \bar{q}_j \quad (i \neq j)$	$\frac{4}{9} \frac{s^2 + u^2}{t^2}$
3	$q_i q_i \rightarrow q_i q_i$	$\frac{4}{9} \left(\frac{s^2 + u^2}{t^2} + \frac{s^2 + t^2}{u^2} \right) - \frac{8}{27} \frac{s^2}{\hat{u}\hat{t}}$
4	$q_i \bar{q}_i \rightarrow q_i \bar{q}_i$	$\frac{4}{9} \left(\frac{s^2 + u^2}{t^2} + \frac{t^2 + u^2}{s^2} \right) - \frac{8}{27} \frac{u^2}{\hat{s}\hat{t}}$
5	$q_i \bar{q}_i \rightarrow gg$	$\frac{32}{27} \frac{u^2 + t^2}{\hat{u}\hat{t}} - \frac{8}{3} \frac{u^2 + t^2}{s^2}$
6	$gg \rightarrow q_i \bar{q}_i$	$\frac{1}{6} \frac{u^2 + t^2}{\hat{u}\hat{t}} - \frac{3}{8} \frac{u^2 + t^2}{s^2}$
7	$q_i g \rightarrow q_i g$	$\frac{4}{9} \frac{u^2 + s^2}{\hat{u}\hat{s}} + \frac{u^2 + s^2}{t^2}$
8	$gg \rightarrow gg$	$\frac{9}{2} \left(3 - \frac{\hat{u}\hat{t}}{s^2} - \frac{\hat{u}\hat{s}}{t^2} - \frac{\hat{s}\hat{t}}{u^2} \right)$

REFERENCES

- (1) CERN-Columbia-Rockefeller and Saclay-Strasbourg collaborations, data contributed to the XVth International Conference on High Energy Physics, Chicago-Batavia, (1972).
- (2) R.P. Feynman, Phys. Rev. Lett. 23, 1415 (1969); J.D. Bjorken and E.A. Paschos, Phys. Rev. 185, 1975 (1969).
- (3) R.P. Feynman, "Photon-Hadron Interactions" (Benjamin, N.Y. 1972).
- (4) S.D. Drell and J.D. Walecka, Ann. Phys. 28, 18 (1964).
- (5) J.D. Bjorken, Phys. Rev. Lett. 16, 408 (1966).
- (6) S.L. Adler, Phys. Rev. 143, 1144 (1966).
- (7) J.D. Bjorken, Phys. Rev. 179, 1547 (1969).
- (8) T.M. Yan, Ann. Rev. Nucl. Sci. 26, 199 (1976); C.H. Llewellyn Smith, in Springer Tracts in Modern Physics ed. by G. Hohler, (Springer-Verlag, 1972), Vol. 62. p. 51.
- (9) S.M. Berman, J.D. Bjorken, and J. Kogut, Phys. Rev. D4, 3388 (1971).
- (10) S.D. Ellis and M.B. Kislinger, Phys. Rev. D9, 2027 (1974).
- (11) F.W. Busser et al. Phys. Lett. 46B, 471 (1973).
- (12) D. Sivers, S.J. Brodsky, and R. Blankenbecler, Phys. Reports 23C, 1 (1976).
- (13) R. Blankenbecler, S.J. Brodsky, and J.F. Gunion, Phys. Rev. D6, 2652 (1972); Phys. Lett. 42B, 461 (1973); R. Blankenbecler and S.J. Brodsky, Phys. Rev. D10, 2973 (1974); J.F. Gunion, Phys. Rev. D10, 242 (1974); R. Blankenbecler, S.J. Brodsky, and J. Gunion, Phys. Rev. D12, 3469 (1975).
- (14) P.V. Landshoff and T.C. Polkinghorne, Phys. Rev. D8, 927 (1973); Phys. Rev. D10, 891 (1974).
- (15) S.J. Brodsky and G.R. Farrar, Phys. Rev. Lett. 31, 1/53 (1973); V.A. Matveev, R.M. Muradyan, and A.N. Tavkhelidze, Lett. Nuovo Cimento 7, 719 (1973); S.J. Brodsky and G.R. Farrar, Phys. Rev. D11, 1309 (1975).
- (16) S.D. Ellis, in "Particles and Fields '77", Proceedings of the Annual Meeting of the Division of Particles and Fields of the APS, Argonne (AIP-1978), p. 271.
- (17) R.D. Field and R.P. Feynman, Phys. Rev. D15, 2590 (1977).

- (18) G.C. Fox, "Phenomenology of High p_T Scattering", Caltech Report No. CALT-68-573 (1976). See also Refs 43 and 74.
- (19) See the review article of Ref. 12 and:
 - a) J.C. Polkinghorne, in Proceedings of the 1977 European Conference on Particle Physics, Budapest, ed. by L. Jenik and J. Montvay (CRIP, Budapest, 1978) Vol. I p. 441.
 - b) S.D. Ellis and R. Stroynowski, Rev. Mod. Phys. 49, 753 (1977);
 - c) M.K. Chase and W.J. Stirling, Nucl. Phys. B133, 157 (1978);
 - d) M. Jacob and P.V. Landshoff, "Large transverse momentum and jet studies" to be published in Phys. Reports.
- (20) K.G. Wilson, Phys. Rev. Lett. 27, 690 (1971).
- (21) J. Kogut and L. Susskind, Phys. Rev. D9, 697 (1974).
- (22) J. Kogut and L. Susskind, Phys. Rev. D9, 3391 (1974).
- (23) D.J. Gross and F. Wilczek, Phys. Rev. Lett. 30, 1343 (1973);
H.D. Politzer, Phys. Rev. Lett. 30, 1346 (1973).
- (24) C.N. Yang and R. Mills, Phys. Rev. 96, 191 (1954).
- (25) A. Zee, Phys. Rev. D7, 3630 (1973); S. Coleman and D.J. Gross, Phys. Rev. Lett. 31, 851 (1973).
- (26) For general reviews of QCD, see:
 - a) H.D. Politzer, Phys. Reports 14C, 129 (1974);
 - b) W. Marciano and H. Pagels, Phys. Reports 36C, 137 (1977);
 - c) J. Ellis, "Deep Hadronic Structure", CERN Report 1977, (Lectures presented at the 1976 Les Houches Summer School).
- (27) C. Chang et al., Phys. Rev. Lett. 35, 901 (1975); E.M. Riordan et al., SLAC Report No. SLAC-PUB-1634 (1975).
- (28) H. Anderson et al., Phys. Rev. Lett. 38, 1450 (1977); W.R. Francis, in "Particles and Fields '77", Proceedings of the Annual Meeting of the Division of Particles and Fields of the APS, Argonne (AIP-1978), p. 339.
- (29) H. Anderson, H.S. Matis and L.C. Myrianthopoulos, Phys. Rev. Lett. 40 1061 (1978); Aachen-Born-CERN-London-Oxford-Saclay Collaboration, "Analysis of Nucleon Structure Functions in CERN Bubble Chamber Neutrino Experiments", Oxford Report 16/78 (1978).
- (30) R.F. Cahalan, K.A. Geer, J. Kogut and L. Susskind, Phys. Rev. D11, 1199 (1975).
- (31) R.C. Hwa, A. Spiessbach, and M. Teper, Phys. Rev. Lett. 36, 1418 (1976).

- (32) A.P. Contogouris, R. Gaskell, and A. Nicolaidis, Progr. Theor. Phys. 58, 1238 (1977); Phys. Rev. D17, 839 (1978); Proceedings of the International Symposium on Multiparticle Dynamics, Kaysersberg, 1977 (Centre de Recherches Nucleaires, Strasbourg, France), p. B-225.
- (33) A.P. Contogouris, R. Gaskell, and A. Nicolaidis, Phys. Rev. D17, 2992 (1978).
- (34) R.C. Hwa, A. Spiessbach, and M. Teper, University of Oregon report, 1977; E. Fischbach and G. Look, Phys. Rev. D15, 2576 (1977); G. Look and E. Fischbach, Phys. Rev. D16, 1369 (1977).
- (35) M. Binkley et al., Phys. Rev. Lett. 37, 574 (1976); K. Anderson et al., Phys. Rev. Lett. 37, 799 (1976); D.C. Hom et al., Phys. Rev. Lett. 37, 1374 (1976).
- (36) L. Lederman, in Proceedings of the 1977 European Conference on Particle Physics, Budapest, ed. by L. Jenik and I. Montvay (CRIP, Budapest, 1978), Vol. I p. 303.
- (37) C.N. Brown, review talk in "Particles and Fields '77", Proceedings of the Annual Meeting of the Division of Particles and Fields of the APS, Argonne (AIP-1978), p. 375; D. Kaplan et al., (Stony Brook-Fermilab-Columbia Collaboration) report, 1977.
- (38) P. Darriulat, Rapporteur review, in Proceedings of the XVII International Conference on High Energy Physics, Tbilisi, 1976, edited by N.N. Bogoliubov et al. (JINR, Dubna, U.S.S.R. 1977), Vol I, p. A4-23; P. Darriulat et al., Nucl. Phys. B107, 429 (1976).
- (39) M. Della Negra et al., Nucl. Phys. B127, 1 (1977).
- (40) H. Boggild, review talk in Proceedings of the VIII International Symposium on Multiparticle Dynamics, Kaysersberg, 1977, (Centre de Research Nucleaires, Strasbourg, France), p. B-1.
- (41) R. Baier and B. Peterson, Univ. of Bielefeld Report No. 77/10.
- (42) M. Fontannaz and D.I. Schiff, Nucl. Phys. B132, 457 (1978).
- (43) R.P. Feynman, R.D. Field, and G.C. Fox, Nucl. Phys. B128, 1 (1977).
- (44) B. Combridge, Phys. Rev. D12, 2893 (1975).
- (45) M.K. Chase, Nucl. Phys. B145, 189 (1978).
- (46) See Ref. 43 and the discussion at the introduction of the second Refs. 78.
- (47) B. Combridge, J. Kripfganz, and J. Ranft, Phys. Lett. B70, 234 (1977); J. Kripfganz, in Proceedings of the VIII International Symposium on

Multiparticle Dynamics, Kayzersberg, 1977 (Centre de Recherches Nucleaires, Strasbourg, France), p. B-253; B. Combridge, in Proceedings of the Workshop on Large $-p_T$ Phenomena, Bielefeld, 1977.

- (48) R. Cutler and D. Sivers, Phys. Rev. D17, 196 (1978).
- (49) J. F. Owens, E. Reya, and M. Glück, Phys. Rev. D18, 1501 (1978).
- (50) A. Buras, Nucl. Phys. B125, 125 (1977).
- (51) A. Buras and K. Gaemers, Nucl. Phys. B132, 249 (1978).
- (52) C.T. Sachrajda, Phys. Lett. 76B, 100 (1978).
- (53) C.T. Sachrajda, in "Phenomenology of Quantum Chromodynamics", Proceedings of the XIII Recontre de Moriond, Flaine, France, 1978 ed. by J. Tran Thanh Van (Editions Frontieres, Paris, 1978), p. 17.
- (54) H.D. Politzer, Nucl. Phys. B129, 301 (1977).
- (55) S.D. Drell and T.M. Yan, Phys. Rev. Lett. 25, 316 (1970); Ann. Phys. 66, 578 (1971).
- (56) C.T. Sachrajda, Phys. Lett. 73B, 185 (1978).
- (57) Y.L. Dokshitzer, D.I. D'yakonov, and S.I. Troyan, SLAC-TRANS-183, Trans. from Proc. of the 13th Leningrad Winter School on Elementary Particle Physics, (1978).
- (58) D. Amati, R. Petronzio, and G. Veneziano, Nucl. Phys. B140, 54 (1978); Nucl. Phys. B146, 29 (1978).
- (59) C.H. Llewellyn Smith, Acta Physica Austriaca, Suppl. XIX, 331 (1978).
- (60) R. Ellis, H. Georgi, M. Machacek, H.D. Politzer and G. Ross, Phys. Lett. 78B, 281 (1978).
- (61) S. Libby and G. Sterman, Phys. Rev. D18, 3252 (1978).
- (62) A.P. Contogouris, R. Gaskell and S. Papadopoulos, Phys. Rev. D17, 2314 (1978).
- (63) See Appendix A of Ref. 12.
- (64) K. Kinoshita et al., Phys. Lett. B68, 355 (1977).
- (65) V.N. Gribov and L.N. Lipatov, Yad. Fiz. 15, 1218 (1972) (Sov. J. Nucl. Phys. 15, 675 (1972)).
- (66) A.M. Polyakov, in Proceedings of the 1975 International Symposium on Lepton and Photon Interactions at High Energies, Stanford, California edited by W.T. Kirk (SLAC, Stanford, 1976), p. 855.

- (67) A.H. Mueller, Phys. Rev. D9, 963 (1974); C. Callan and M. Goldberger, Phys. Rev. D11, 1611 (1975).
- (68) J.F. Owens, Phys. Lett. 76B, 85 (1978).
- (69) G. Altarelli and G. Parisi, Nucl. Phys. B126, 298 (1977).
- (70) See Refs. 52, 53 and 60.
- (71) D.J. Gross, Phys. Rev. Lett. 32, 1071 (1974).
- (72) D.G. Cassel, in "Particles and Fields '77", Proceedings of the Annual Meeting of the Division of Particles and Fields of the APS, Argonne (AIP-1978), p. 297.
- (73) J. Ranft and G. Ranft, Lett. Nuovo Cimento 20, 669 (1977).
- (74) R.P. Feynman, Caltech Report No. CALT-68-588, (1977).
- (75) E.M. Levin and M.G. Ryskin, Leningrad Report No. 280, (1976).
- (76) G. Altarelli, G. Parisi and R. Petronzio, Phys. Lett. 76B, 356 (1978); R. Petronzio, CERN-TH-2495 (1978).
- (77) F. Halzen, in Proceedings of the 19th International Conference on High Energy Physics, Tokyo, 1978 (Physical Society of Japan, 1979), p. 214.
- (78) R.D. Field, in Proceedings of the 19th International Conference on High Energy Physics, Tokyo, 1978, (Physical Society of Japan, 1979), p.743; Caltech Report No. CALT-68-672 (1978).
- (79) G. Altarelli, G. Parisi and R. Petronzio, Phys. Lett. 76B, 351 (1978).
- (80) K. Kajantie and R. Raitio, Nucl. Phys. B139, 72 (1978); K. Kajantie, J. Lindfors, and R. Raitio, Helsinki Report No. HU-TFT-78-18 (1978).
- (81) F. Halzen and D. Scott, Phys. Rev. Lett. 40, 1117 (1978); Phys. Rev. D18, 3378 (1978); H. Fritzsch and P. Minkowski, Phys. Lett. 73B, 80 (1978).
- (82) A.P. Contogouris, R. Gaskell and S. Papadopoulos, Nuovo Cimento (in press); Proceedings of the IX International Symposium on High Energy Multiparticle Dynamics, 1978, (Tabor, Czechoslovakia) p. D-61.
- (83) B. Pope, in "Particles and Fields '77", Proceedings of the Annual Meeting of the Division of Particles and Fields of the APS, Argonne (AIP-1978), p. 239.
- (84) C. Kourkouvelis et al., (Athens-Brookhaven-CERN-Suracuse-Yale Collaboration), "Inclusive π^0 production at very large p_T at ISR" CERN report 1978.

- (85) G. Parisi and R. Petronzio, Phys. Lett. 62B, 331 (1976).
- (86) I. Hinchliffe and C.H. Llewellyn Smith, Phys. Lett. 66B, 281 (1977).
- (87) G.R. Farrar, Nucl. Phys. 77B, 429 (1974); J.F. Gunion, Phys. Rev. D10, 242 (1974).
- (88) A.P. Contogouris and R. Gaskell, Nucl. Phys. B126, 157 (1977).
- (89) R.P. Feynman, R.D. Field, and G.C. Fox, Phys. Rev. D18, 3320 (1978).
- (90) R.D. Field, Phys. Rev. Lett. 40, 997 (1978).
- (91) J.F. Owens and J.O. Kimel, Phys. Rev. D18, 3313 (1978).
- (92) J. Ranft and G. Ranft, Karl-Marx University Report No. KMU-HEP-78-06 (1978)
- (93) W.E. Caswell, R.R. Horgan, and S.J. Brodsky, Phys. Rev. D18, 2415 (1978).
- (94) S.J. Brodsky, SLAC Report No. SLAC-PUB-2217 (1978).
- (95) R. Blankenbecler, S.J. Brodsky and J.F. Gunion, Phys. Rev. D18, 900 (1978).
- (96) J.F. Gunion, "High Transverse Momentum Physics in Quantum Chromodynamics" Report of University of California, Davis (1978).
- (97) D. Jones and J.F. Gunion, Phys. Rev. D19, 867 (1979).
- (98) M.G. Albrow, et al., Niels Bohr Institute Report (1978); K.H. Hansen, in Proceedings of the 19th International Conference on High Energy Physics, Tokyo, 1978, (Physical Society of Japan, 1979), p. 177; Nucl. Phys. B135, 461 (1978).
- (99) D. Antreasyan, et al., Phys. Lett. 38, 112 (1977); and Report No. EFI 78-29 (1979).
- (100) R. Baier, J. Cleymans, K. Kinoshita and B. Peterseon, Nucl. Phys. B118, 139 (1977).
- (101) L. Sehgal, Nucl. Phys. B90, 471 (1975).
- (102) P.V. Landshoff, J.C. Polkinghorne, and R.D. Short, Nucl. Phys. B28, 222 (1971); S.J. Brodsky, F.E. Close, and J.F. Gunion, Phys. Rev. D8, 3678 (1973).
- (103) K. Kinoshita and Y. Kinoshita, Progr. Theor. Phys. 60 No. 5 (1978)
R. Raitio and R. Sosnowski, University of Helsinki Report No. HU-TFT-77-22 (1977).
- (104) S.R. Horgan and P.N. Scharbach, Phys. Lett. 81B, 215 (1979).

- (105) E. Bloom and F. Gilman, Phys. Rev. D4, 2901 (1971).
- (106) O. Nachtman, Nucl. Phys. B63, 237 (1973); B78, 455 (1974); H. Georgi and H.D. Politzer, Phys. Rev. D14, 1829 (1976).
- (107) K. Eggert et al., Nucl. Phys. B98, 49 (1975).
- (108) B. Alper et al., Nucl. Phys. B100, 237 (1975).
- (109) D. C. Carey et al., Fermilab Reports No. 75/20 and 75/25-Exp.
- (110) G. Donaldson et al., Phys. Rev. Lett. 36, 1100 (1976).
- (111) J.W. Cronin et al., Phys. Rev. D11, 3105 (1975).
- (112) A. Clark, P. Darriulat et al., Phys. Lett. 74B, 267 (1978).

FIGURE CAPTIONS

- Figure 1. Inelastic electron-hadron scattering in the one-photon exchange approximation.
- Figure 2. Large p_{\perp} hadron production in hadronic collisions. The large transverse momentum reaction $A + B \rightarrow C + X$ is assumed to occur as a result of a single large angle scattering of constituents $a + b \rightarrow c + d$, followed by the fragmentation of c into the observed particle C .
- Figure 3. — Lowest order graphs contributing to the subprocesses:
 (a) $qq \rightarrow qq$, (b) $q\bar{q} \rightarrow q\bar{q}$, (c) $qg \rightarrow qg$, (d) $gg \rightarrow q\bar{q}$,
 (e) $gg \rightarrow gg$.
 The graphs contributing to the subprocess $q\bar{q} \rightarrow gg$ are similar to those in (d) and have been omitted.
- Figure 4. Separate contributions to $pp \rightarrow \pi^0 + X$ and $pp \rightarrow \frac{1}{2}(\pi^+ + \pi^-) + X$ at $\theta = 90^\circ$ of the subprocesses $qq \rightarrow qq$, $qg \rightarrow qg$, $gg \rightarrow gg$.
- Figure 5. Inclusive cross sections for $pp \rightarrow \pi^0 + X$ and $pp \rightarrow \frac{1}{2}(\pi^+ + \pi^-) + X$ at $\theta = 90^\circ$. Data: \diamond Ref. 83, \square 107, \blacksquare 108, \circ 109, \triangle 110, \blacktriangle 111, \bullet 112.
- Figure 6. As in Fig. 5 for nonscaling quark $G_{C/c} = G_{C/c}(z, Q^2)$.
- Figure 7. As in Fig. 5 with $\gamma = 3$ and $\gamma = 10$ (without k_T effects).

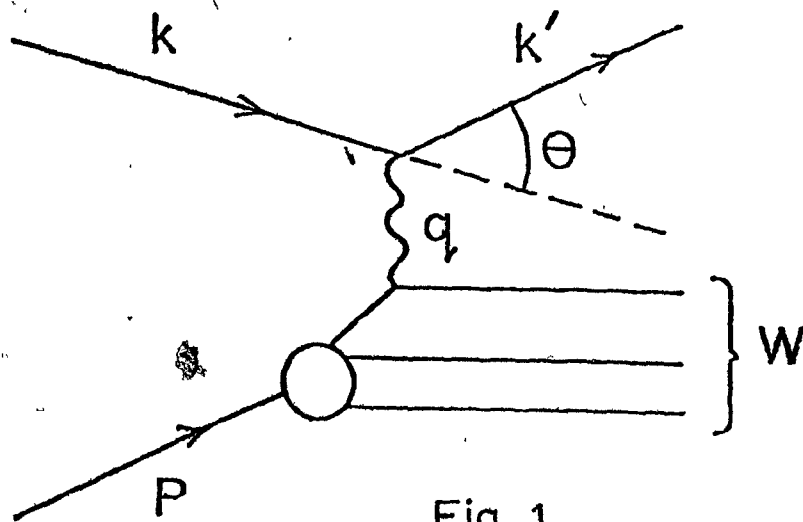


Fig. 1

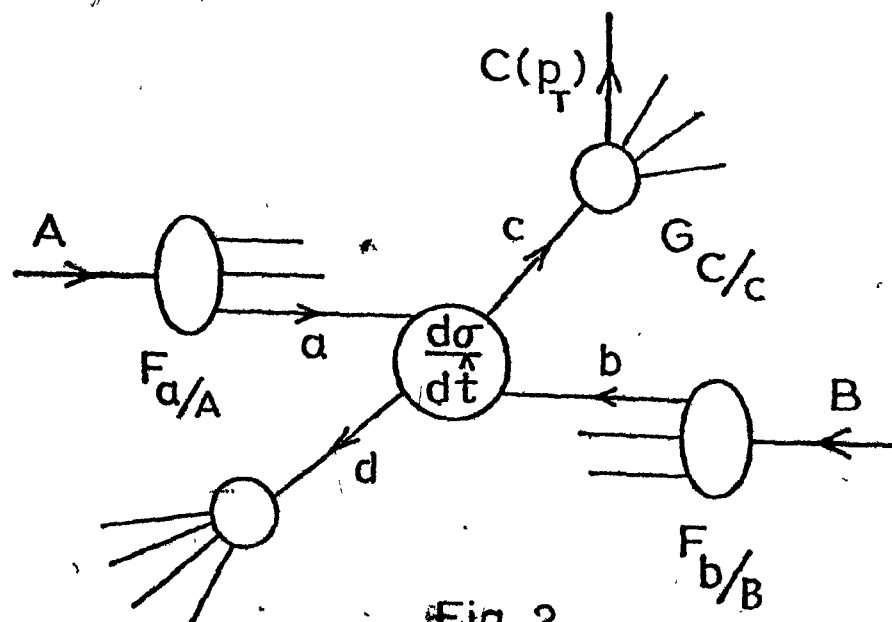
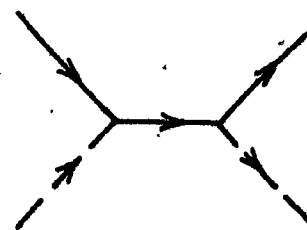
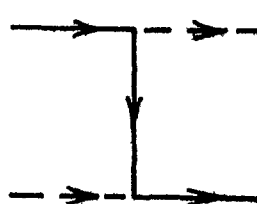
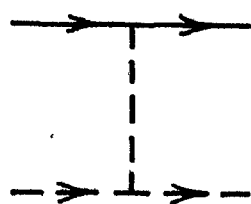
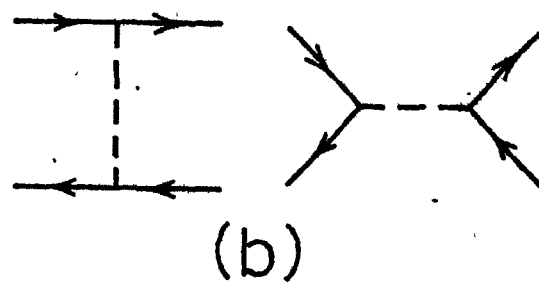
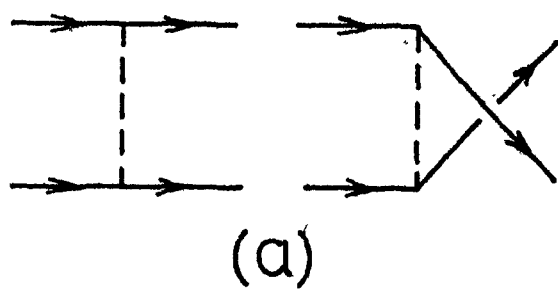
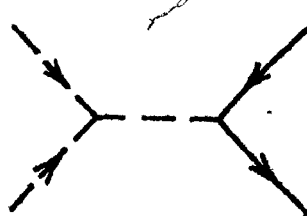
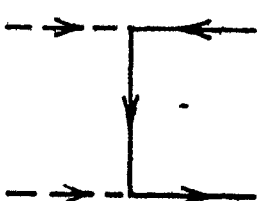
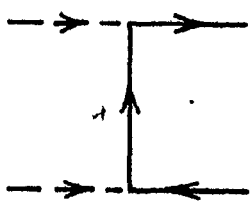


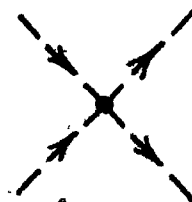
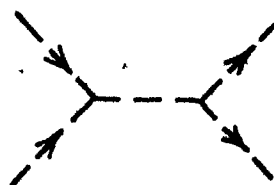
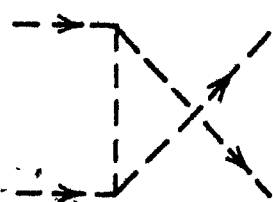
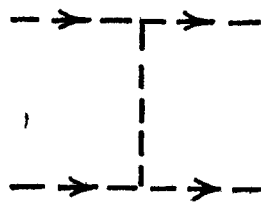
Fig. 2



(c)



(d)



(e)

Fig.3

O

$$\sqrt{s} = 52.7 \text{ GeV}$$

$$\text{cm}^2 \text{ GeV}^{-2} \quad G_{c/c} = G_{c/c}(z), \quad \gamma = 5$$

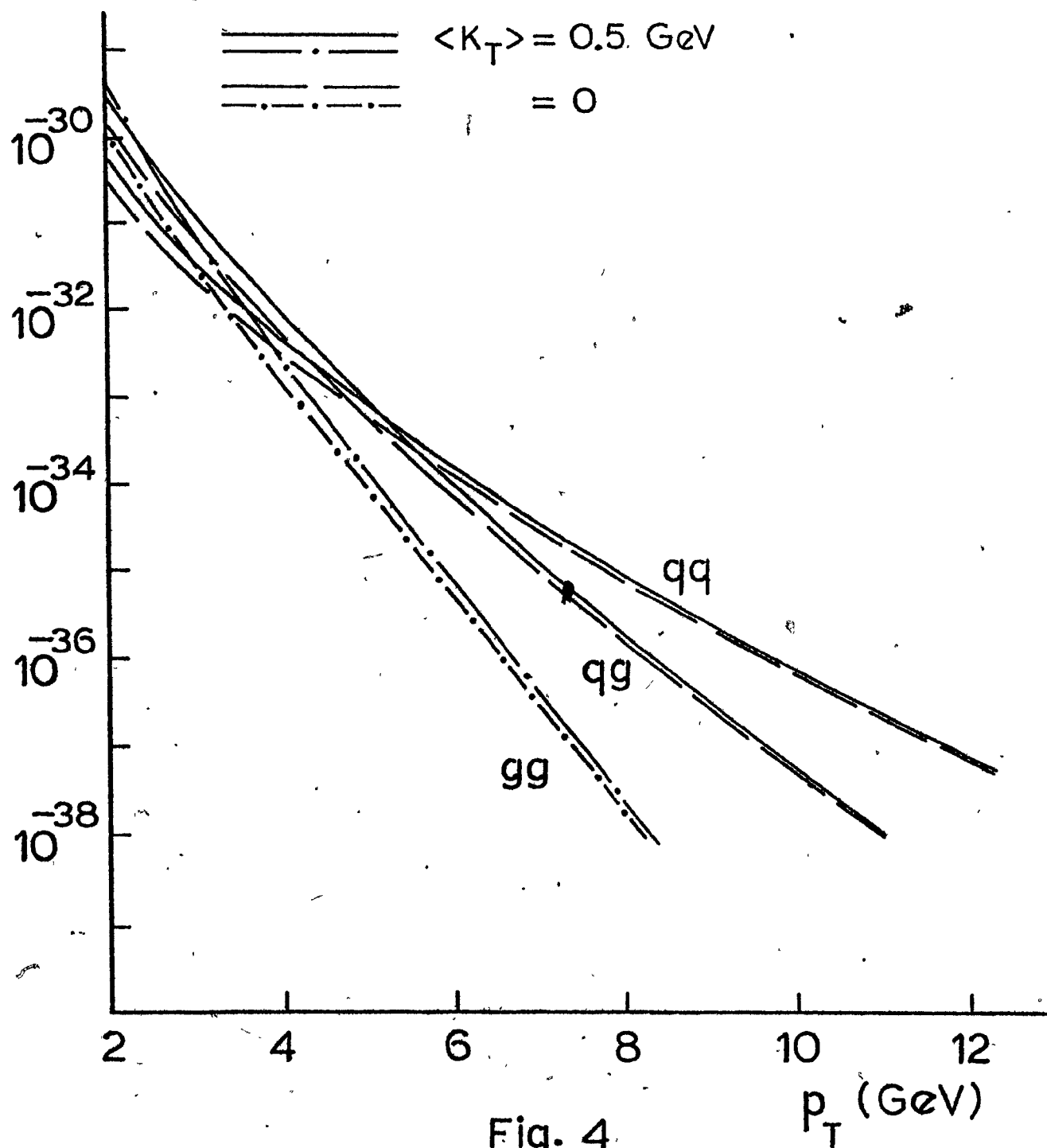
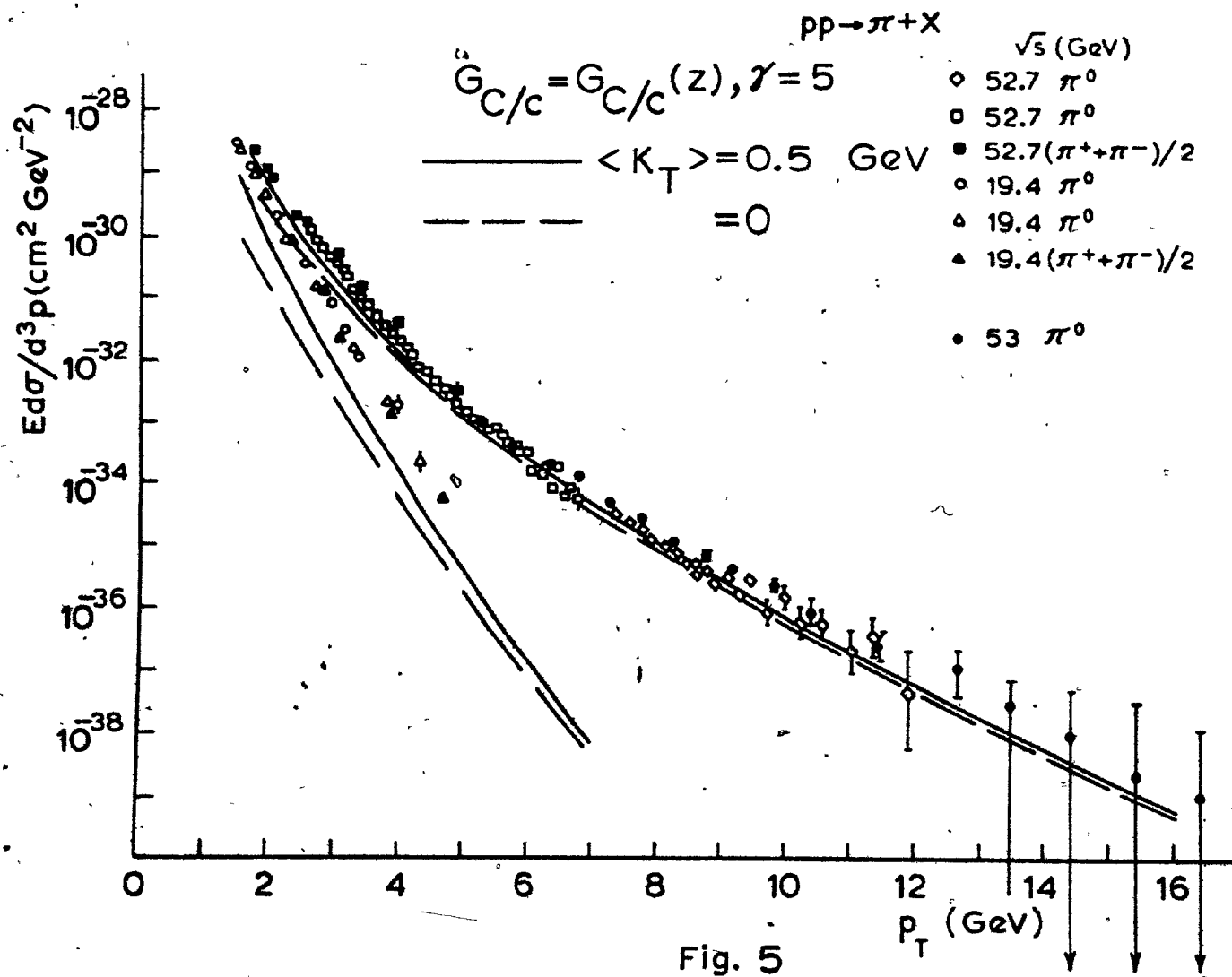


Fig. 4



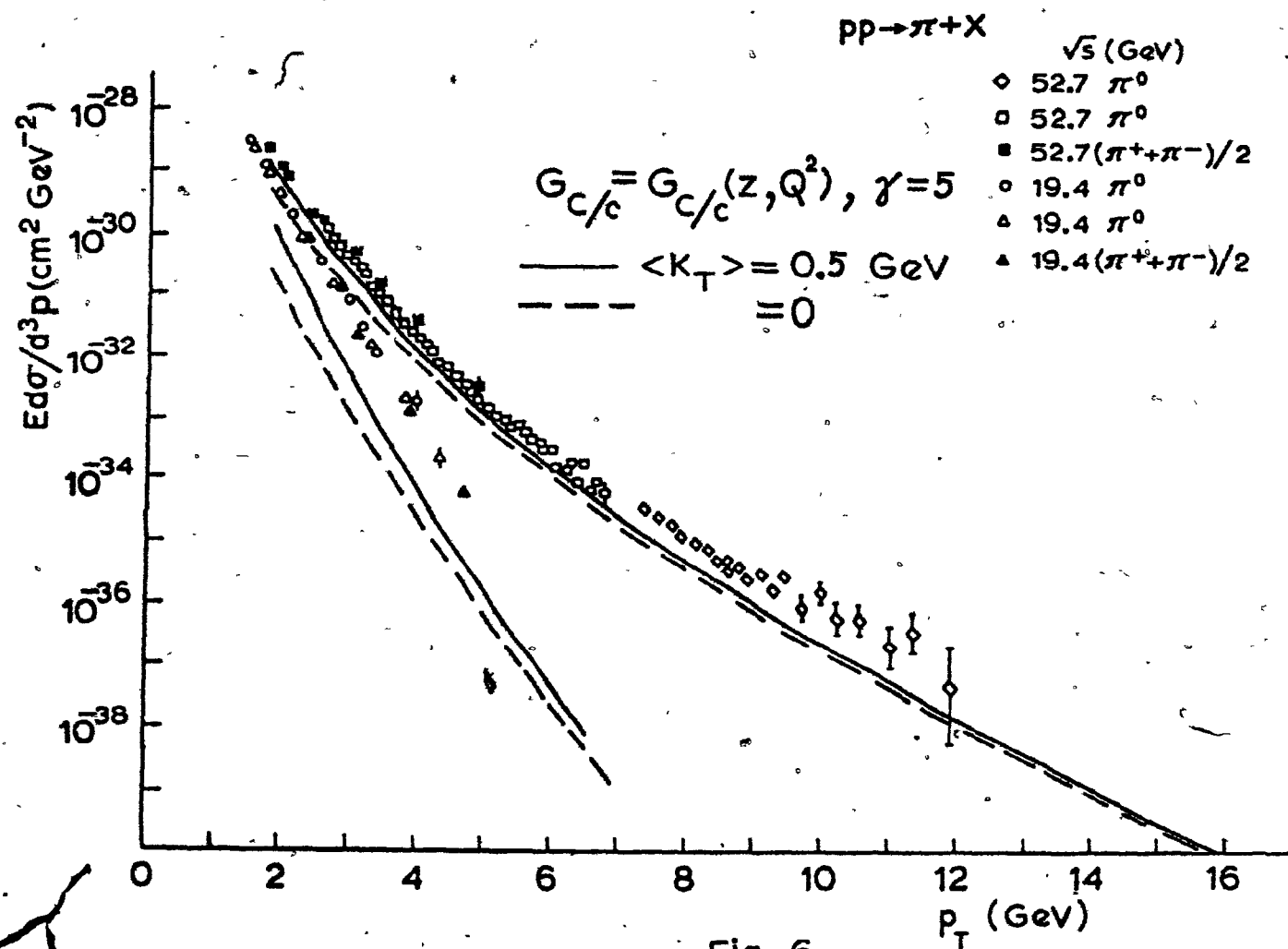


Fig. 6

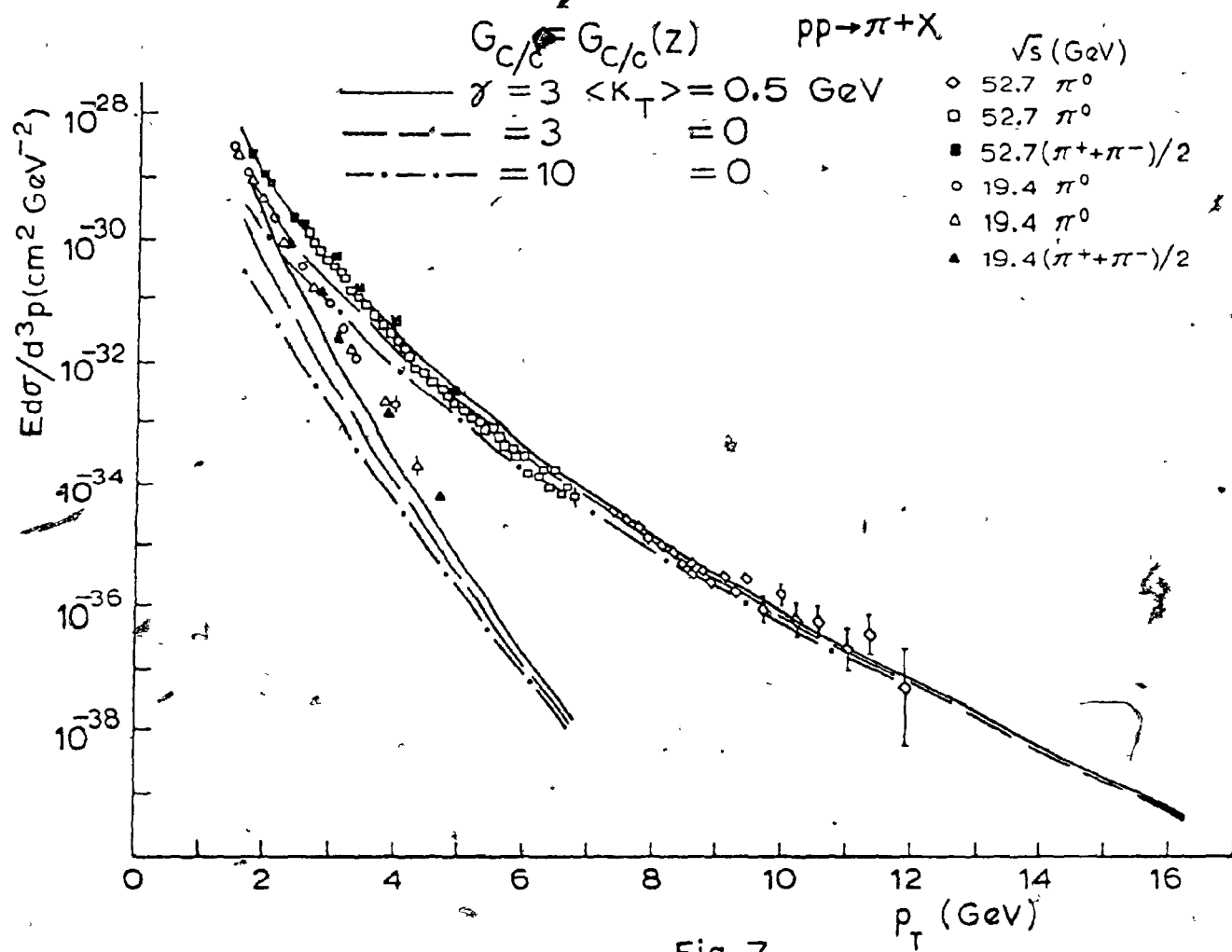


Fig. 7